

An aerial photograph of a river system in a forested basin. The river is a vibrant greenish-blue color, winding through a dense forest of evergreen trees. The river has several meanders and a large loop in the center. The surrounding land is a mix of green forest and brownish, possibly cleared or agricultural areas. The sky is clear and blue.

**REMOTE SENSING DATA COLLECTION:**  
**Flathead Basin, MT**  
March 29<sup>th</sup>, 2010

**Submitted to:**

**Stephen Story**  
**Montana DNRC**  
**Water Resources Division**  
**1424 9<sup>th</sup> Ave.**  
**Helena, MT 59620-1601**

**Submitted by:**

**Watershed Sciences**  
**257B SW Madison Ave.**  
**Corvallis, OR 97333**  
**529 SW 3rd Ave. Suite 300**  
**Portland, Oregon 97204**





# REMOTE SENSING DATA COLLECTION:

## AIRBORNE DATA ACQUISITION AND PROCESSING:

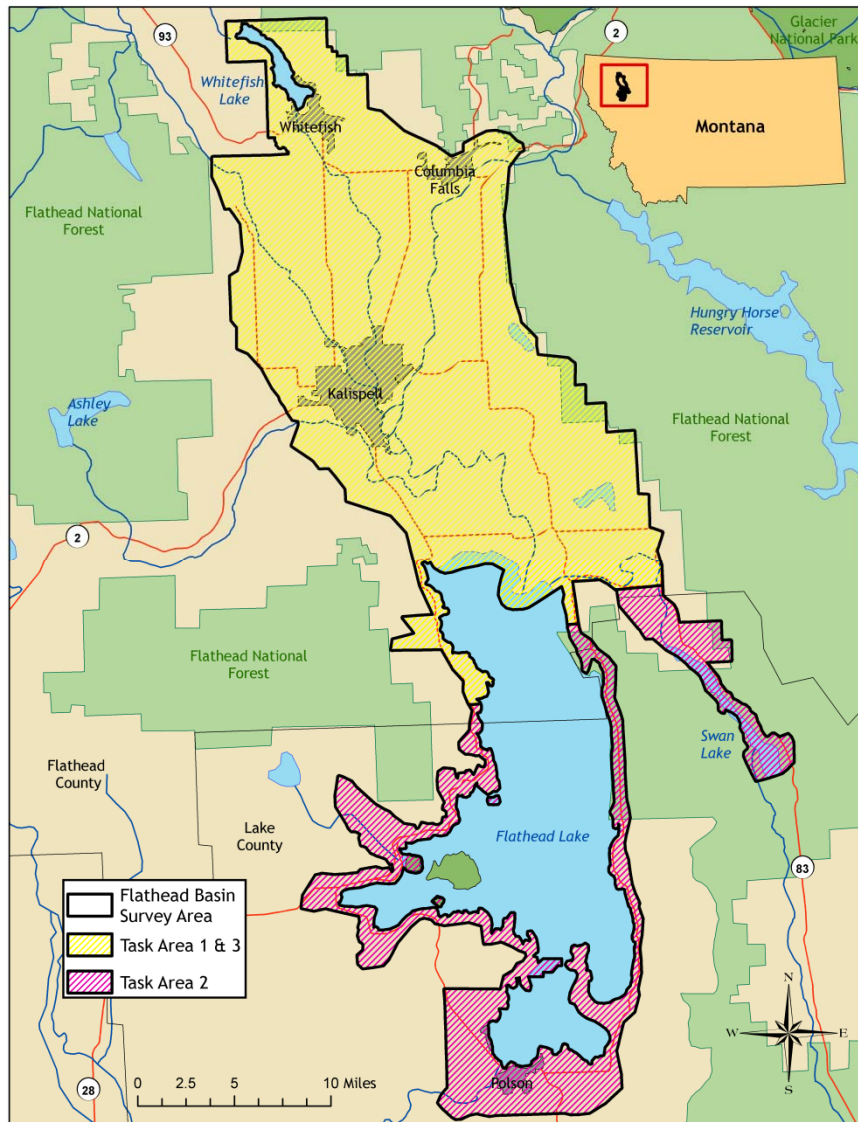
### FLATHEAD BASIN, MONTANA

|   |    |
|---|----|
| 1. Overview .....                                       | 1  |
| 2. LiDAR Acquisition .....                              | 2  |
| 2.1 Airborne Survey - Instrumentation and Methods ..... | 2  |
| 2.2 Ground Survey - Instrumentation and Methods.....    | 3  |
| 2.2.1 Survey Control.....                               | 3  |
| 2.2.2 RTK Survey.....                                   | 4  |
| 3. LiDAR Data Processing .....                          | 6  |
| 3.1 Applications and Work Flow Overview.....            | 6  |
| 3.2 Aircraft Kinematic GPS and IMU Data.....            | 6  |
| 3.3 Laser Point Processing.....                         | 7  |
| 4. LiDAR Accuracy Assessment.....                       | 8  |
| 4.1 Laser Noise and Relative Accuracy .....             | 8  |
| 4.2 Absolute Accuracy.....                              | 9  |
| 5. Study Area Results.....                              | 9  |
| 5.1 LiDAR Data Summary .....                            | 9  |
| 5.2 LiDAR Data Density/Resolution .....                 | 9  |
| 5.3 LiDAR Relative Accuracy Calibration Results .....   | 13 |
| 5.4 LiDAR Absolute Accuracy.....                        | 14 |
| 5.5 Projection/Datum and Units .....                    | 17 |
| 6. Orthophoto Processing and Results .....              | 17 |
| 6.1 Processing .....                                    | 17 |
| 6.2 Accuracy .....                                      | 19 |
| 7. Hydrologically Enforced Terrain Model.....           | 19 |
| 8. Contours.....  | 22 |
| 9. Deliverables .....                                   | 23 |
| 10. Selected Images .....                               | 24 |
| 11. Glossary.....                                       | 33 |
| 12. Citations .....                                     | 34 |
| Appendix A.....   | 35 |
| Appendix B.....   | 36 |
| Appendix C.....   | 37 |

# 1. Overview

Watershed Sciences, Inc. (WS) acquired Light Detection and Ranging (LiDAR) data of Montana's Flathead Basin from September 22 - 29, 2009. The original requested survey area (303,040 acres) was expanded to include a 100m buffer to ensure complete coverage and adequate point densities around survey area boundaries. Additionally, from September 23 - 25, 2009 orthorectified true-color (RGB) and color infrared (NIR) imagery was collected and then processed by 3Di West (GeoTerra Mapping Group) based in Eugene, Oregon. The survey area has been divided into 3 task areas. Task Area 2 was delivered first, followed by Task Area 1&3. This final report and delivery cover the entire Flathead Basin survey area as a whole. The total area of delivered LiDAR for the Flathead Basin, including the 100 m buffer, is 321,049 acres. The total area of delivered orthophotographs is 518,208 acres.

Figure 1. Flathead Basin Project survey area



Remote Sensing Data Acquisition and Processing: Flathead Basin, Montana

Prepared by Watershed Sciences, Inc.



## 2. LiDAR Acquisition

### 2.1 Airborne Survey - Instrumentation and Methods

The LiDAR survey uses a Leica ALS50 Phase II laser system. For the Flathead Basin survey site, the sensor scan angle was  $\pm 15^\circ$  from nadir<sup>1</sup> with a pulse rate designed to yield an average native density (number of pulses emitted by the laser system) of  $\geq 4$  points per square meter over terrestrial surfaces. All survey areas were surveyed with an opposing flight line side-lap of  $\geq 50\%$  ( $\geq 100\%$  overlap) to reduce laser shadowing and increase surface laser painting. The Leica ALS50 Phase II system allows up to four range measurements (returns) per pulse, and all discernable laser returns were processed for the output dataset. It is not uncommon for some types of surfaces (e.g. dense vegetation or water) to return fewer pulses than the laser originally emitted. These discrepancies between ‘native’ and ‘delivered’ density will vary depending on terrain, land cover and the prevalence of water bodies.

To accurately solve for laser point position (geographic coordinates x, y, z), the positional coordinates of the airborne sensor and the attitude of the aircraft were recorded continuously throughout the LiDAR data collection mission. Aircraft position was measured twice per second (2 Hz) by an onboard differential GPS unit. Aircraft attitude was measured 200 times per second (200 Hz) as pitch, roll and yaw (heading) from an onboard inertial measurement unit (IMU). To allow for post-processing correction and calibration, aircraft/sensor position and attitude data are indexed by GPS time.



*The Cessna Caravan is a stable platform, ideal for flying slow and low for high density projects. The Leica ALS50 sensor head installed in the Caravan is shown on the left.*



---

<sup>1</sup> Nadir refers to the perpendicular vector to the ground directly below the aircraft. Nadir is commonly used to measure the angle from the vector and is referred to a “degrees from nadir”.

## 2.2 Ground Survey - Instrumentation and Methods

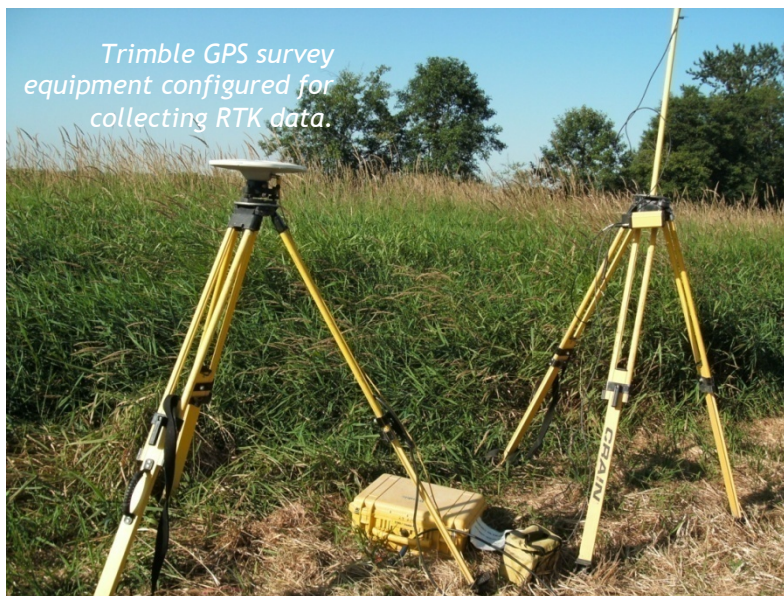
The following ground survey data were collected to enable the geo-spatial correction of the aircraft positional coordinate data collected throughout the flight, and to allow for quality assurance checks on final LiDAR data products.

### 2.2.1 Survey Control

Montana Professional Land Surveyor (PLS) Andy Belski, of River Design Group, MT, located and certified all survey monuments, air targets, and ground checkpoints used for both LiDAR and orthophoto data collections. The survey control plan was designed to provide redundant control within 13 nautical miles of the mission area for LiDAR flights. The controls were set prior to the airborne missions with survey control coordinates established using an extensive GPS network. (**Appendix C**)

Simultaneous with the airborne data collection mission, we conducted multiple static (1 Hz recording frequency) ground surveys over monuments with known coordinates (**Table 1**). Indexed by time, these GPS data are used to correct the continuous onboard measurements of aircraft position recorded throughout the mission. After the airborne survey, these static GPS data were then processed using triangulation with Continuously Operating Reference Stations (CORS) stations, and checked against the Online Positioning User Service (OPUS<sup>2</sup>) to confirm antenna height measurements and reported position accuracy.

Certified controls were also measured for 4-band imagery processing (aerial target control points) and are included in **Table 1**.



---

<sup>2</sup> Online Positioning User Service (OPUS) is run by the National Geodetic Survey to process corrected monument positions.



Table 1. Base Station and aerial target survey control coordinates for the Flathead Basin survey area established by Montana PLS, Andy Belski.

| Monument ID | Description            | Datum: NAD83 (CORS91) |                     | GRS80                |
|-------------|------------------------|-----------------------|---------------------|----------------------|
|             |                        | Latitude              | Longitude           | Ellipsoid Z (meters) |
| 2000        | WF Airport             | 48° 24'36.47915" N    | 114° 18'30.39731" W | 913.70               |
| 2001        | WF Airport (secondary) | 48° 24'36.28566" N    | 114° 18'30.53178" W | 913.87               |
| 2002        | NGS F 422              | 48° 07'01.42707" N    | 114° 15'20.60613" W | 871.75               |
| 2003        | NGS F 422 (secondary)  | 48° 07'01.58321" N    | 114° 15'20.54662" W | 871.86               |
| 2004        | Ferndale (primary)     | 48° 03'05.74842" N    | 114° 00'21.65367" W | 919.23               |
| 2005        | Ferndale (secondary)   | 48° 03'05.75942" N    | 114° 00'22.51189" W | 919.20               |
| 2007        | K 443                  | 47° 50'08.06192" N    | 114° 20'07.84518" W | 881.85               |
| 2008        | NGS Z 443              | 47° 43'54.37511" N    | 114° 12'58.82530" W | 927.68               |
| 2009        | NGS A 444              | 47° 43'17.49697" N    | 114° 12'16.06767" W | 891.22               |
| 2010        | SV-08                  | 47° 52'42.73083" N    | 114° 01'45.00981" W | 887.93               |
| 2011        | SV-12                  | 47° 41'04.86871" N    | 114° 04'14.44625" W | 879.47               |
| 2012        | SV-11                  | 47° 44'50.41685" N    | 114° 13'50.03322" W | 1029.34              |
| 2013        | SV-10                  | 47° 49'36.34566" N    | 114° 21'08.11760" W | 876.41               |
| 2014        | SV-02                  | 48° 24'51.60839" N    | 114° 17'11.14315" W | 928.88               |
| 2015        | SV-03                  | 48° 21'34.95439" N    | 114° 09'14.19312" W | 926.35               |
| 2016        | SV-04                  | 48° 17'53.63403" N    | 114° 25'43.28965" W | 940.37               |
| 2017        | SV-01                  | 48° 28'39.21779" N    | 114° 26'00.83321" W | 900.58               |
| 2018        | SV-09                  | 47° 56'09.69683" N    | 113° 51'08.24309" W | 924.27               |
| 2019        | SV-06                  | 48° 08'59.77185" N    | 114° 05'03.44287" W | 909.30               |
| 2020        | SV-07                  | 48° 00'53.08824" N    | 114° 14'58.89186" W | 923.81               |
| 2121        | SV-05                  | 48° 12'40.56239" N    | 114° 13'46.47019" W | 878.81               |
| 2023        | NGS A507 (secondary)   | 48° 18'20.91574" N    | 114° 15'01.56654" W | 886.979              |

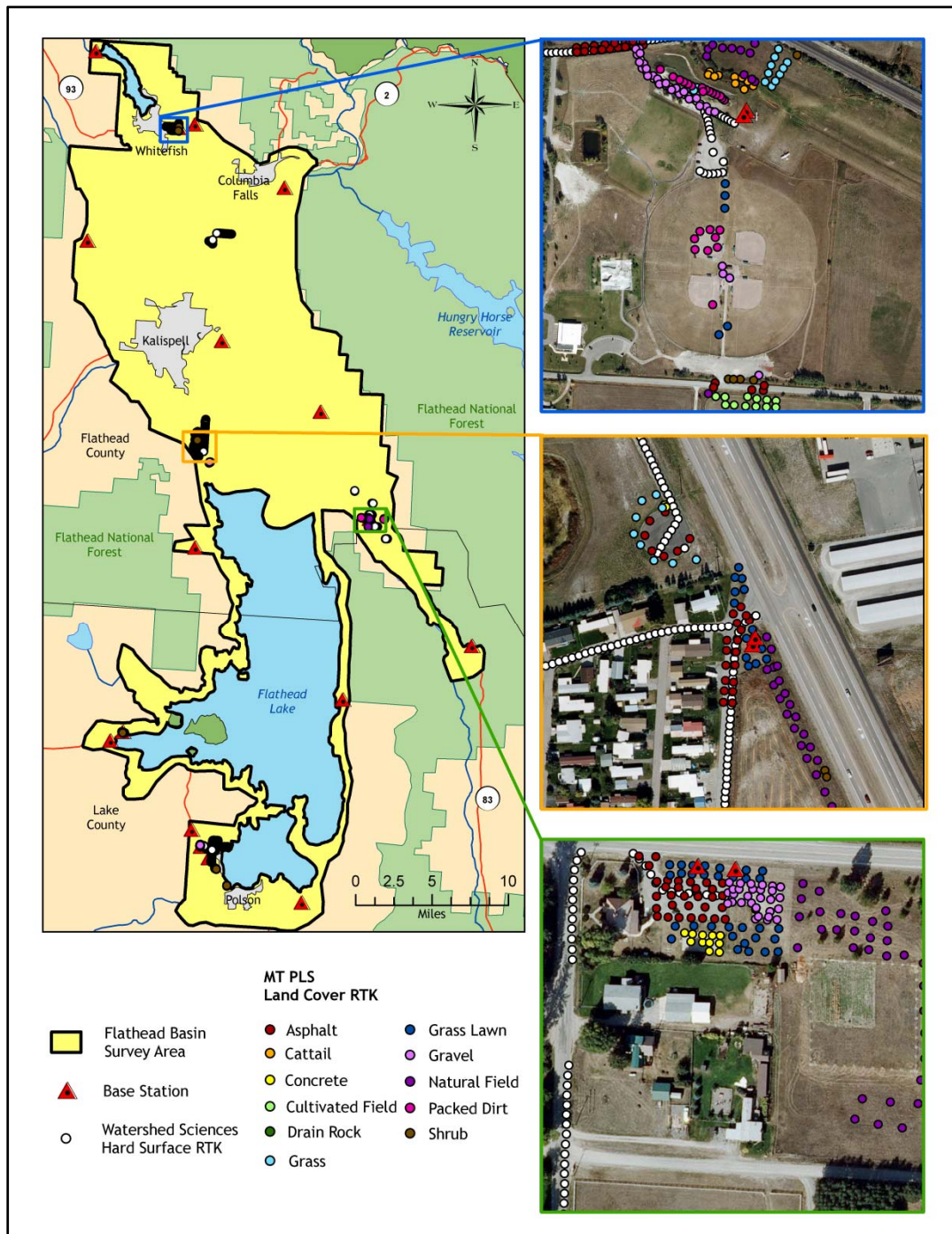
### 2.2.2 RTK Survey

To enable assessment of LiDAR data accuracy, ground truth points were collected using GPS based real-time kinematic (RTK) surveying. This allows for precise location measurements with an error ( $\sigma$ ) of  $\leq 1.5$  cm (0.6 in). For an RTK survey, the ground crew uses a roving unit to receive radio-relayed corrected positional coordinates for all ground points from a GPS base station set up over a survey control monument (PLS certified). Instrumentation includes multiple Trimble DGPS units (R8).

Andrew Belski, MT PLS of River Design Group, Inc., collected RTK points to compare absolute accuracy amongst various land cover types. These ground check points were spatially distributed throughout the survey area in accordance with FEMA guidelines. These data are presented in **Table 3. (Appendix C)**

Watershed Sciences, Inc. collected hard surface RTK points during the LiDAR missions for relative accuracy assessment and to further assess LiDAR point accuracy. All RTK points were corrected using monuments established by Andrew Belski, MT PLS. Figure 2 below portrays a distribution of all RTK point locations used for the survey area.

Figure 2. RTK and base station locations used for the Flathead Basin survey area.



## Remote Sensing Data Acquisition and Processing: Flathead Basin, Montana

Prepared by Watershed Sciences, Inc.



## 3. LiDAR Data Processing

### 3.1 Applications and Work Flow Overview

1. Resolved kinematic corrections for aircraft position data using kinematic aircraft GPS and static ground GPS data.  
**Software:** Waypoint GPS v.8.10, Trimble Geomatics Office v.1.62
2. Developed a smoothed best estimate of trajectory (SBET) file that blends post-processed aircraft position with attitude data. Sensor head position and attitude were calculated throughout the survey. The SBET data were used extensively for laser point processing.  
**Software:** IPAS v.1.35
3. Calculated laser point position by associating SBET position to each laser point return time, scan angle, intensity, etc. Created raw laser point cloud data for the entire survey in \*.las (ASPRS v1.2) format, converting to orthometric elevations (NAVD88) by applying a Geoid03 correction.  
**Software:** ALS Post Processing Software v.2.69
4. Imported raw laser points into manageable blocks (less than 500 MB) to perform manual relative accuracy calibration and filter for pits/birds. Ground points were then classified for individual flight lines (to be used for relative accuracy testing and calibration).  
**Software:** TerraScan v.9.001
5. Using ground classified points per each flight line, the relative accuracy was tested. Automated line-to-line calibrations were then performed for system attitude parameters (pitch, roll, heading), mirror flex (scale) and GPS/IMU drift. Calibrations were performed on ground classified points from paired flight lines. Every flight line was used for relative accuracy calibration.  
**Software:** TerraMatch v.9.001
6. Position and attitude data were imported. Resulting data were classified as ground and non-ground points. Statistical absolute accuracy was assessed via direct comparisons of ground classified points to ground RTK survey data. Ground models were created as a triangulated surface and exported as ArcInfo ASCII grids at a 3-foot pixel resolution. Ground models were also produced at a 6-foot pixel resolution implementing breaklines to hydrologically enforce the model.  
**Software:** TerraScan v.9.001, ArcMap v9.3, TerraModeler v.9.001
7. Model keypoints were selected from a subset of ground-classified points based upon the requested contour interval and desired spatial tolerance. The 2 ft. interval contours were then created from these model keypoints in .dxf file format, and exported as feature classes in Arcmap.  
**Software:** TerraScan v.9.001, ArcMap v. 9.3.1, TerraModeler v.9.001

### 3.2 Aircraft Kinematic GPS and IMU Data

LiDAR survey datasets were referenced to the 1 Hz static ground GPS data collected over pre-surveyed monuments with known coordinates. While surveying, the aircraft collected 2 Hz kinematic GPS data, and the onboard inertial measurement unit (IMU) collected 200 Hz aircraft attitude data. Leica IPAS Suite was used to process the kinematic corrections for the aircraft. The static and kinematic GPS data were then post-processed after the survey to

---

Remote Sensing Data Acquisition and Processing: Flathead Basin, Montana

obtain an accurate GPS solution and aircraft positions. IPAS v.1.35 was used to develop a trajectory file that includes corrected aircraft position and attitude information. The trajectory data for the entire flight survey session were incorporated into a final smoothed best estimated trajectory (SBET) file that contains accurate and continuous aircraft positions and attitudes.

### 3.3 Laser Point Processing

Laser point coordinates were computed using the IPAS and ALS Post Processor software suites based on independent data from the LiDAR system (pulse time, scan angle), and aircraft trajectory data (SBET). Laser point returns (first through fourth) were assigned an associated (x, y, z) coordinate along with unique intensity values (0-255). The data were output into large LAS v. 1.2 files; each point maintains the corresponding scan angle, return number (echo), intensity, and x, y, z (easting, northing, and elevation) information.

These initial laser point files were too large for subsequent processing. To facilitate laser point processing, bins (polygons) were created to divide the dataset into manageable sizes (< 500 MB). Flightlines and LiDAR data were then reviewed to ensure complete coverage of the survey area and positional accuracy of the laser points.

Laser point data were imported into processing bins in TerraScan, and manual calibration was performed to assess the system offsets for pitch, roll, heading and scale (mirror flex). Using a geometric relationship developed by Watershed Sciences, each of these offsets was resolved and corrected if necessary.

LiDAR points were then filtered for noise, pits (artificial low points), and birds (true birds as well as erroneously high points) by screening for absolute elevation limits, isolated points and height above ground. Each bin was then manually inspected for remaining pits and birds and spurious points were removed. In a bin containing approximately 7.5-9.0 million points, an average of 50-100 points are typically found to be artificially low or high. Common sources of non-terrestrial returns are clouds, birds, vapor, haze, decks, brush piles, etc.

Internal calibration was refined using TerraMatch. Points from overlapping lines were tested for internal consistency and final adjustments were made for system misalignments (i.e., pitch, roll, heading offsets and scale). Automated sensor attitude and scale corrections yielded 3-5 cm improvements in the relative accuracy. Once system misalignments were corrected, vertical GPS drift was then resolved and removed per flight line, yielding a slight improvement (<1 cm) in relative accuracy.

The TerraScan software suite is designed specifically for classifying near-ground points (Soininen, 2004). The processing sequence began by 'removing' all points that were not 'near' the earth based on geometric constraints used to evaluate multi-return points. The resulting bare earth (ground) model was visually inspected and additional ground point modeling was performed in site-specific areas to improve ground detail. This manual editing of grounds often occurs in areas with known ground modeling deficiencies, such as: bedrock outcrops, cliffs, deeply incised stream banks, and dense vegetation. In some cases, automated ground point classification erroneously included known vegetation (i.e., understory, low/dense shrubs, etc.). These points were manually reclassified as non-grounds.



Ground surface rasters were developed from triangulated irregular networks (TINs) of ground points.

## 4. LiDAR Accuracy Assessment

Our LiDAR quality assurance process uses the data from the real-time kinematic (RTK) ground survey conducted in the survey area. In the Flathead Basin, a total of **4229 RTK GPS** measurements were collected on hard surfaces distributed among multiple flight swaths. To assess absolute accuracy, we compared the location coordinates of these known RTK ground survey points to those calculated for the closest laser points. As an additional measure of accuracy, RTK points were collected by Andrew Belski, PLS of River Design Group, Inc., in various land cover types. A comparison of check points against ground classified LiDAR points is summarized by land cover class in **Table 3 (also see Appendix C)**.

### 4.1 Laser Noise and Relative Accuracy

Laser point absolute accuracy is largely a function of laser noise and relative accuracy. To minimize these contributions to absolute error, we first performed a number of noise filtering and calibration procedures prior to evaluating absolute accuracy.

#### *Laser Noise*

For any given target, laser noise is the breadth of the data cloud per laser return (i.e., last, first, etc.). Lower intensity surfaces (roads, rooftops, still/calm water) experience higher laser noise. The laser noise range for this survey was approximately 0.02 meters.

#### *Relative Accuracy*

Relative accuracy refers to the internal consistency of the data set - the ability to place a laser point in the same location over multiple flight lines, GPS conditions, and aircraft attitudes. Affected by system attitude offsets, scale, and GPS/IMU drift, internal consistency is measured as the divergence between points from different flight lines within an overlapping area. Divergence is most apparent when flight lines are opposing. When the LiDAR system is well calibrated, the line-to-line divergence is low (<10 cm). See Appendix A for further information on sources of error and operational measures that can be taken to improve relative accuracy.

### Relative Accuracy Calibration Methodology

1. Manual System Calibration: Calibration procedures for each mission require solving geometric relationships that relate measured swath-to-swath deviations to misalignments of system attitude parameters. Corrected scale, pitch, roll and heading offsets were calculated and applied to resolve misalignments. The raw divergence between lines was computed after the manual calibration was completed and reported for each survey area.
2. Automated Attitude Calibration: All data were tested and calibrated using TerraMatch automated sampling routines. Ground points were classified for each individual flight line and used for line-to-line testing. System misalignment offsets (pitch, roll and heading) and scale were solved for each individual mission and applied to respective

mission datasets. The data from each mission were then blended when imported together to form the entire area of interest.

3. **Automated Z Calibration:** Ground points per line were utilized to calculate the vertical divergence between lines caused by vertical GPS drift. Automated Z calibration was the final step employed for relative accuracy calibration.

## 4.2 Absolute Accuracy

The vertical accuracy of the LiDAR data is described as the mean and standard deviation (sigma ~  $\sigma$ ) of divergence of LiDAR point coordinates from RTK ground survey point coordinates. To provide a sense of the model predictive power of the dataset, the root mean square error (RMSE) for vertical accuracy is also provided. These statistics assume the error distributions for x, y, and z are normally distributed, thus we also consider the skew and kurtosis of distributions when evaluating error statistics. Statements of statistical accuracy apply to fixed terrestrial surfaces only and may not be applied to areas of dense vegetation or steep terrain.

## 5. Study Area Results

Summary statistics for point resolution and accuracy (relative and absolute) of the LiDAR data collected in the Flathead Basin survey area are presented below in terms of central tendency, variation around the mean, and the spatial distribution of the data (for point resolution by bin).

### 5.1 LiDAR Data Summary

*Table 2. Resolution and Accuracy - Specifications and Achieved Values*

|  | Targeted                       | Achieved   |
|--|--------------------------------|--|
| <b>Resolution:</b>                                 | $\geq 4$ points/m <sup>2</sup> | 4.93 points/m <sup>2</sup><br>(0.46 points/ft <sup>2</sup> ) |
| <b>*Vertical Accuracy (1 <math>\sigma</math>):</b> | <15 cm                         | 3 cm<br>(0.11 ft)  |

\* Based on 4229 hard-surface control points

### 5.2 LiDAR Data Density/Resolution

Some types of surfaces (i.e., dense vegetation, breaks in terrain, steep slopes, water) may return fewer pulses (delivered density) than the laser originally emitted (native density). The first return laser point density of 4.93 points/m<sup>2</sup> exceeds the target of 4 points/m<sup>2</sup> despite some inclusion of water in the form of lakes and lake edges. The first return point map in **Figure 5** identifies native point density by tile.

---

Remote Sensing Data Acquisition and Processing: Flathead Basin, Montana



Ground classifications were derived from automated ground surface modeling and manual, supervised classifications where it was determined that the automated model had failed. Ground return densities will be lower in areas of dense vegetation, water, or buildings. The ground-classified point map in **Figure 6** identifies ground return densities by tile.

**Data Resolution for the Flathead Basin Project survey area:**

- Average First Return Density = 4.93/m<sup>2</sup> (0.46/ft<sup>2</sup>)
- Average Ground Point Density = 1.55/m<sup>2</sup> (0.14/ft<sup>2</sup>)

*Figure 3. Density distribution for first return laser points*

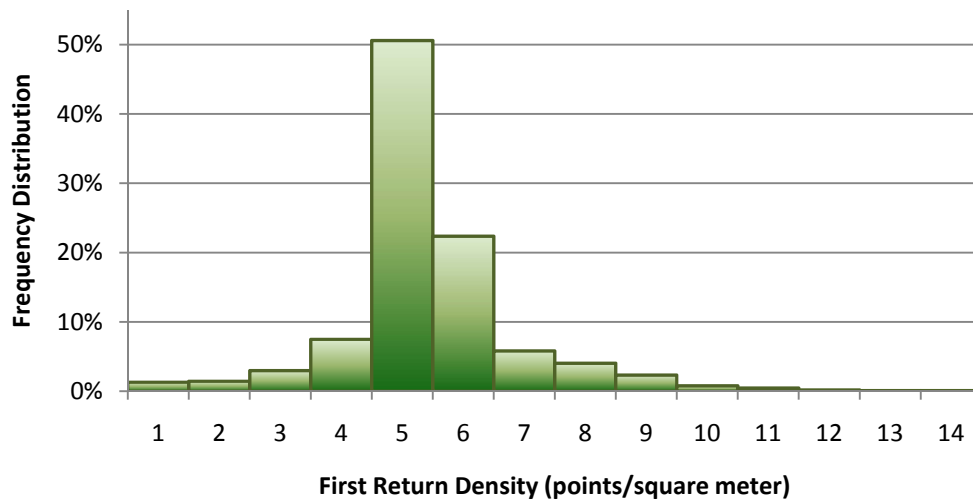


*Figure 4. Density distribution for ground-classified laser points.*

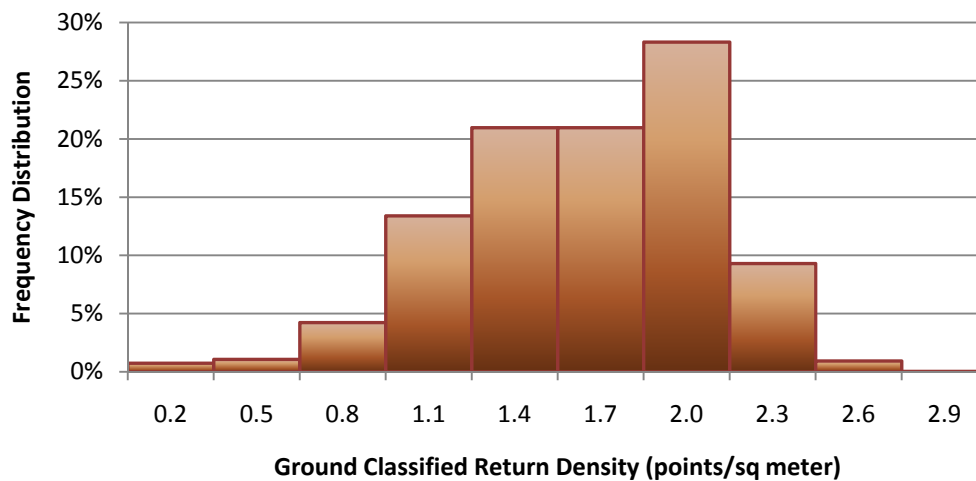


Figure 5. First return laser point density per tile.

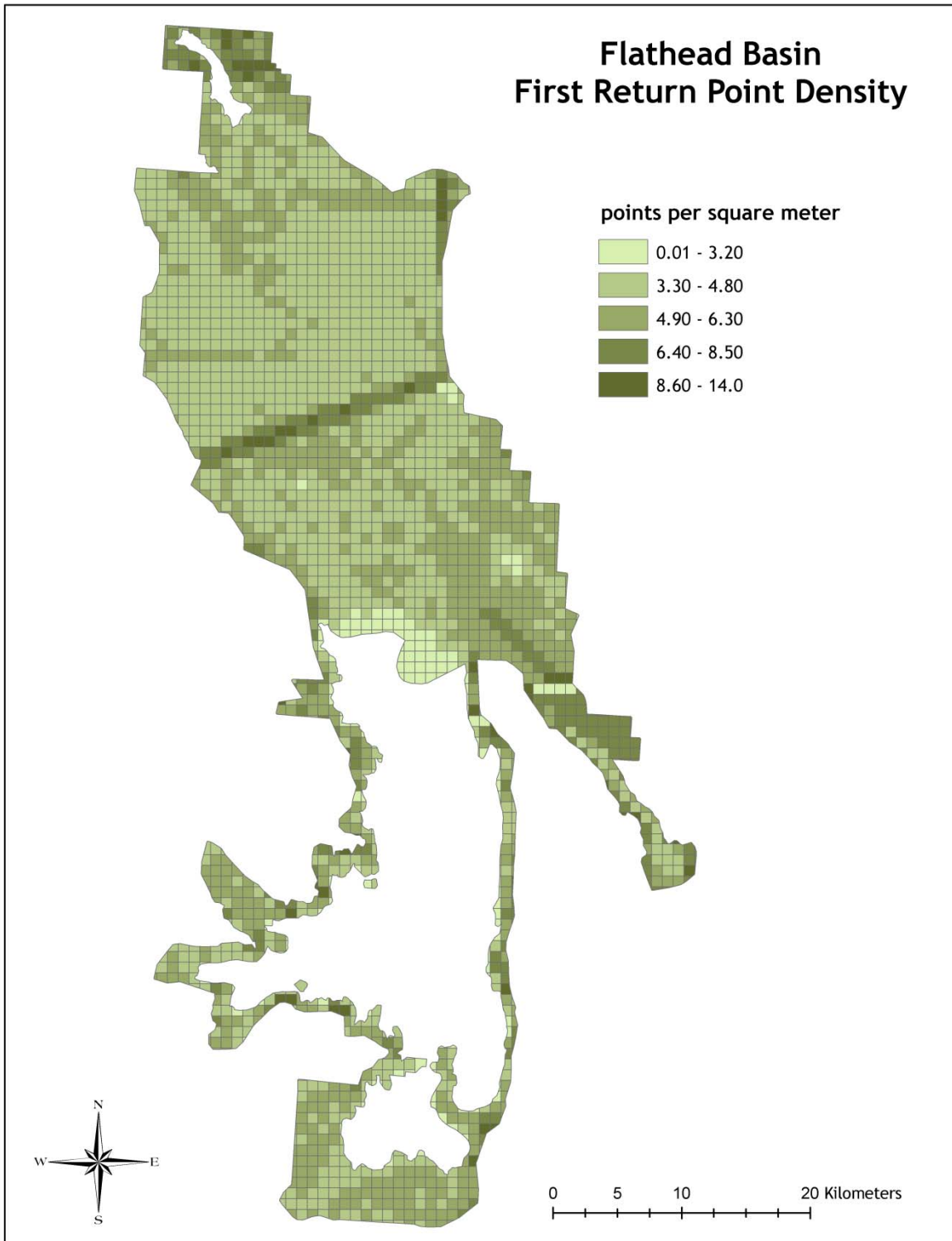
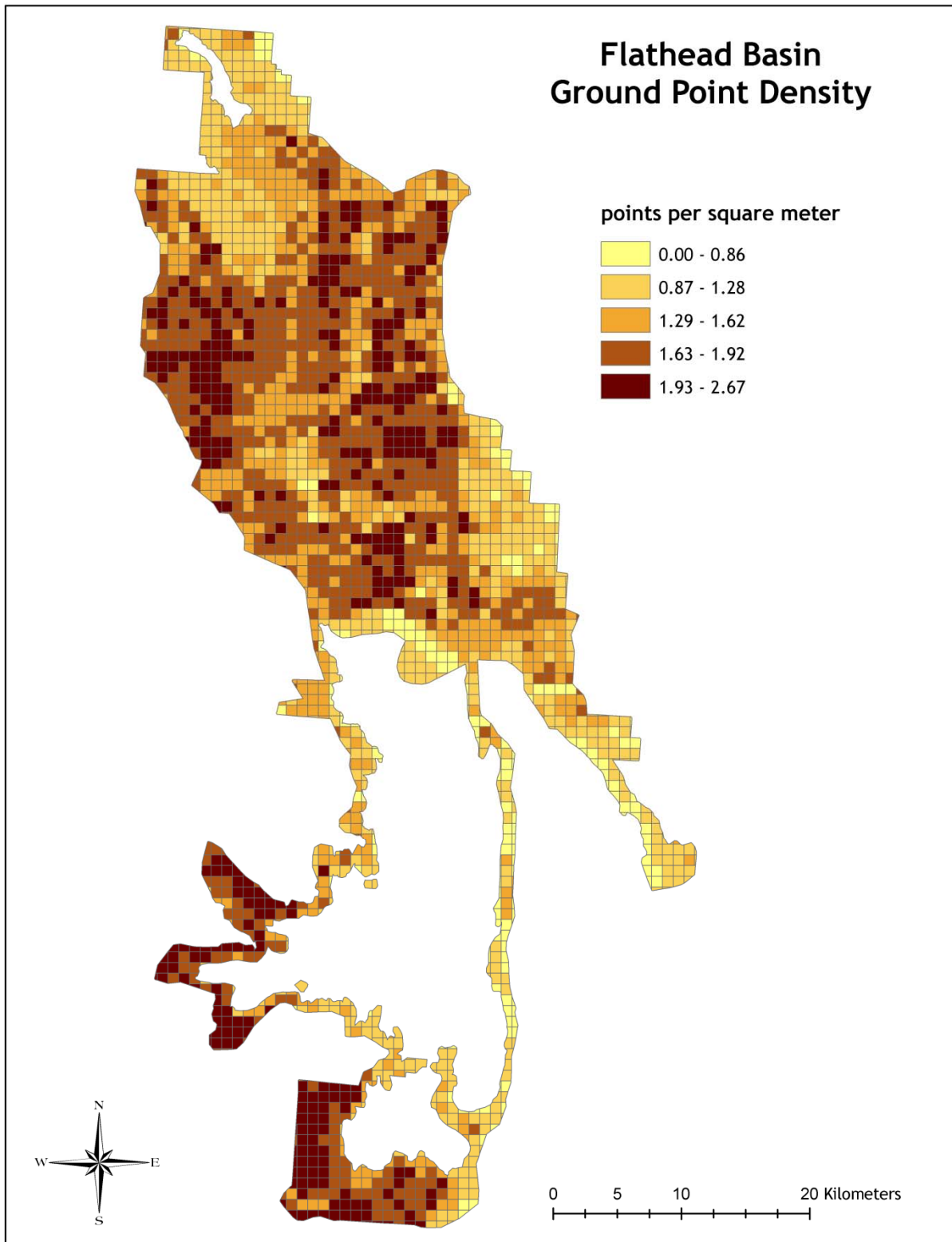


Figure 6. Ground-classified laser point density per tile.



Remote Sensing Data Acquisition and Processing: Flathead Basin, Montana

Prepared by Watershed Sciences, Inc.

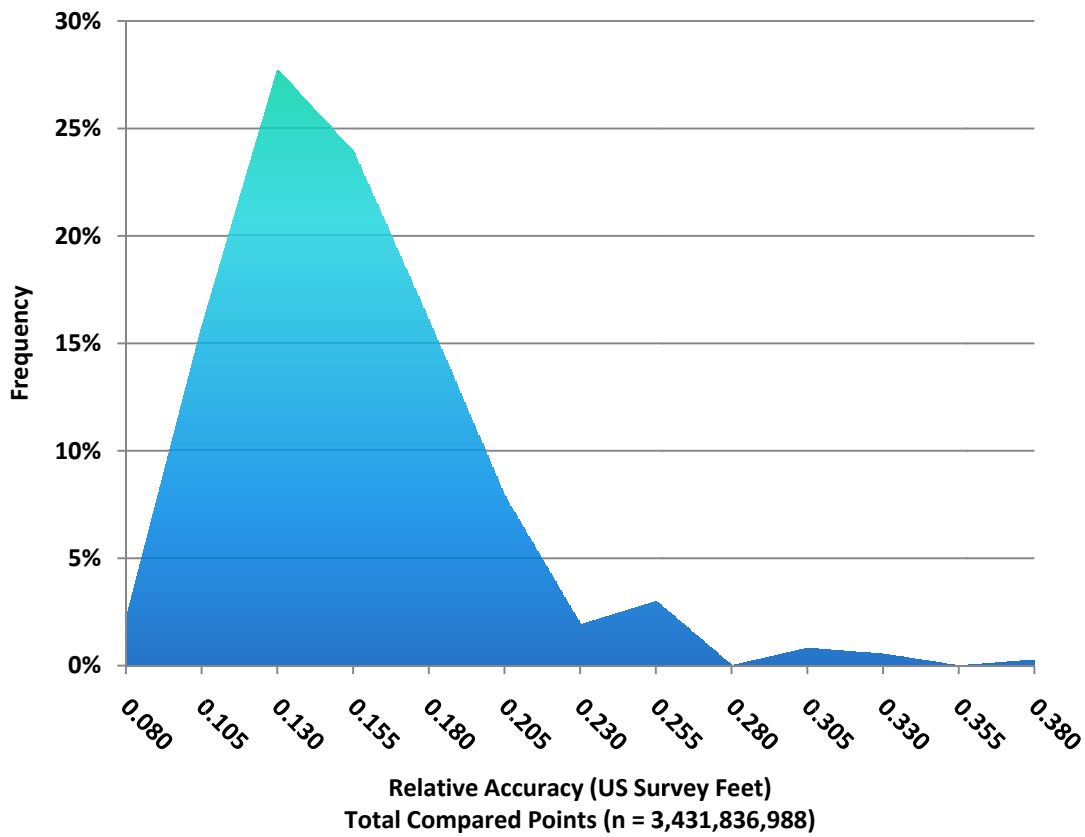


### 5.3 LiDAR Relative Accuracy Calibration Results

Relative accuracies for the Flathead Basin project survey area:

- Project Average = 0.14 ft (0.04 m)
- Median Relative Accuracy = 0.13 ft (0.04 m)
- $1\sigma$  Relative Accuracy = 0.15 ft (0.05 m)
- $2\sigma$  Relative Accuracy = 0.21 ft (0.07 m)

Figure 7. Distribution of relative accuracies per flight line, non slope-adjusted



## 5.4 LiDAR Absolute Accuracy

Absolute accuracies for the Flathead Basin survey area. FEMA checkpoints were collected by Andy Belski, MT PLS, of River Design Group, Inc. Ground cover classes were categorized into predominant cover types with a minimum sample size of 20.

Table 3. Absolute Accuracy - Deviation between laser points and RTK survey points

| RTK Surface Type                  | RTK Survey Sample Size (n) | Root Mean Square Error (RMSE) | Standard Deviations   |                       | Minimum $\Delta z$      | Maximum $\Delta z$    | Average $\Delta z$      |
|-----------------------------------|----------------------------|-------------------------------|-----------------------|-----------------------|-------------------------|-----------------------|-------------------------|
|                                   |                            |                               | 1 sigma ( $\sigma$ )  | 2 sigma ( $\sigma$ )  |                         |                       |                         |
| Hard-surface (Watershed Sciences) | 4229                       | 0.118 ft<br>(0.036 m)         | 0.112 ft<br>(0.034 m) | 0.237 ft<br>(0.072 m) | -0.474 ft<br>(-0.144 m) | 0.596 ft<br>(0.182 m) | 0.008 ft<br>(0.002 m)   |
| Asphalt (MT PLS)                  | 168                        | 0.141 ft<br>(0.043 m)         | 0.155 ft<br>(0.047 m) | 0.256 ft<br>(0.078 m) | -0.329 ft<br>(-0.100 m) | 0.271 ft<br>(0.083 m) | -0.040 ft<br>(-0.012 m) |
| Cattails (MT PLS)                 | 27                         | 1.037 ft<br>(0.316 m)         | 1.075 ft<br>(0.328 m) | 1.396 ft<br>(0.425 m) | 0.273 ft<br>(0.083 m)   | 1.659 ft<br>(0.506 m) | 1.000 ft<br>(0.304 m)   |
| Concrete (MT PLS)                 | 42                         | 0.226 ft<br>(0.069 m)         | 0.229 ft<br>(0.070 m) | 0.428 ft<br>(0.131 m) | -0.567 ft<br>(-0.173 m) | 0.338 ft<br>(0.103 m) | -0.115 ft<br>(-0.035 m) |
| Cultivated Field (MT PLS)         | 92                         | 0.164 ft<br>(0.050 m)         | 0.144 ft<br>(0.044 m) | 0.352 ft<br>(0.108 m) | -0.068 ft<br>(-0.021m)  | 0.408 ft<br>(0.124 m) | 0.119 ft<br>(0.036 m)   |
| Drain Rock (MT PLS)               | 28                         | 0.178 ft<br>(0.054 m)         | 0.215 ft<br>(0.066 m) | 0.275 ft<br>(0.084 m) | -0.187 ft<br>(-0.057 m) | 0.276 ft<br>(0.084 m) | 0.100 ft<br>(0.030 m)   |
| Grass (MT PLS)                    | 49                         | 0.282 ft<br>(0.086 m)         | 0.251 ft<br>(0.077 m) | 0.545 ft<br>(0.166 m) | -0.193 ft<br>(-0.059 m) | 0.619 ft<br>(0.189 m) | 0.206 ft<br>(0.063 m)   |
| Grass, Lawn (MT PLS)              | 109                        | 0.161 ft<br>(0.049 m)         | 0.158 ft<br>(0.048 m) | 0.331 ft<br>(0.101 m) | -0.232 ft<br>(-0.071 m) | 0.370 ft<br>(0.113 m) | 0.066 ft<br>(0.020 m)   |
| Gravel (MT PLS)                   | 174                        | 0.178 ft<br>(0.054 m)         | 0.165 ft<br>(0.050 m) | 0.350 ft<br>(0.107 m) | -0.291 ft<br>(-0.089 m) | 0.437 ft<br>(0.133 m) | 0.074 ft<br>(0.023 m)   |

| RTK Surface Type       | RTK Survey Sample Size (n) | Root Mean Square Error (RMSE) | Standard Deviations   |                       | Minimum $\Delta z$      | Maximum $\Delta z$    | Average $\Delta z$    |
|------------------------|----------------------------|-------------------------------|-----------------------|-----------------------|-------------------------|-----------------------|-----------------------|
|                        |                            |                               | 1 sigma ( $\sigma$ )  | 2 sigma ( $\sigma$ )  |                         |                       |                       |
| Natural Field (MT PLS) | 110                        | 0.392 ft<br>(0.120 m)         | 0.413 ft<br>(0.126 m) | 0.712 ft<br>(0.217 m) | -0.356 ft<br>(-0.109 m) | 0.953 ft<br>(0.290 m) | 0.279 ft<br>(0.085 m) |
| Packed Dirt (MT PLS)   | 57                         | 0.204 ft<br>(0.062 m)         | 0.176 ft<br>(0.054 m) | 0.401 ft<br>(0.122 m) | -0.354 ft<br>(-0.108 m) | 0.455 ft<br>(0.139 m) | 0.046 ft<br>(0.014 m) |
| Shrubs (MT PLS)        | 22                         | 0.570 ft<br>(0.174 m)         | 0.611 ft<br>(0.186 m) | 0.911 ft<br>(0.278 m) | -0.658 ft<br>(-0.201 m) | 0.936 ft<br>(0.285 m) | 0.262 ft<br>(0.080 m) |



Figure 8. Absolute Accuracy - Histogram Statistics, based on 4,229 hard surface points.

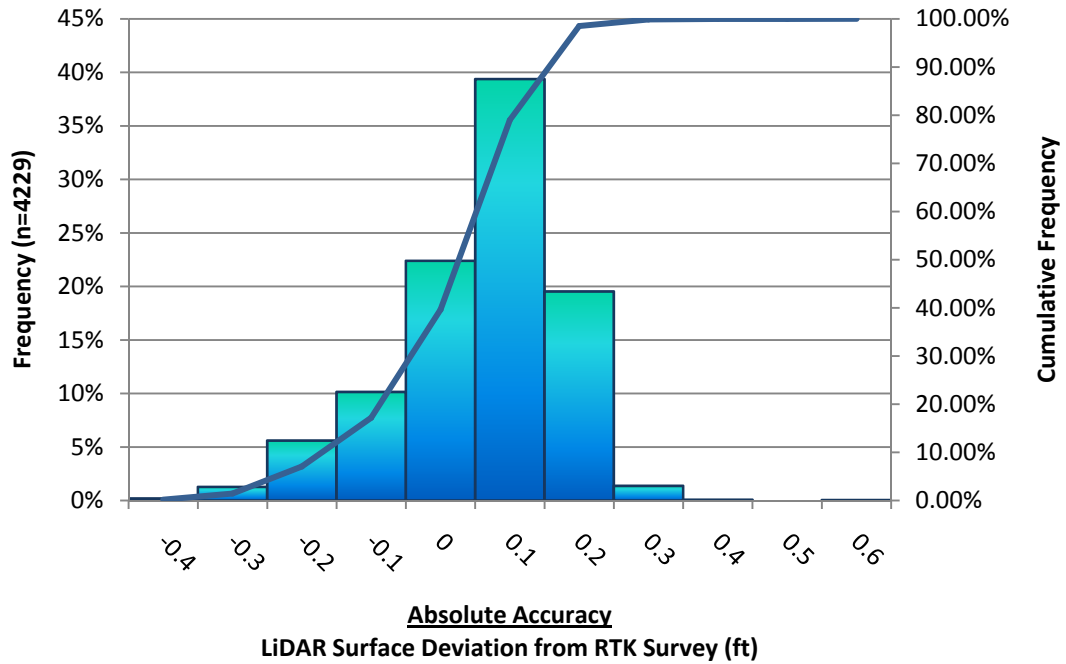
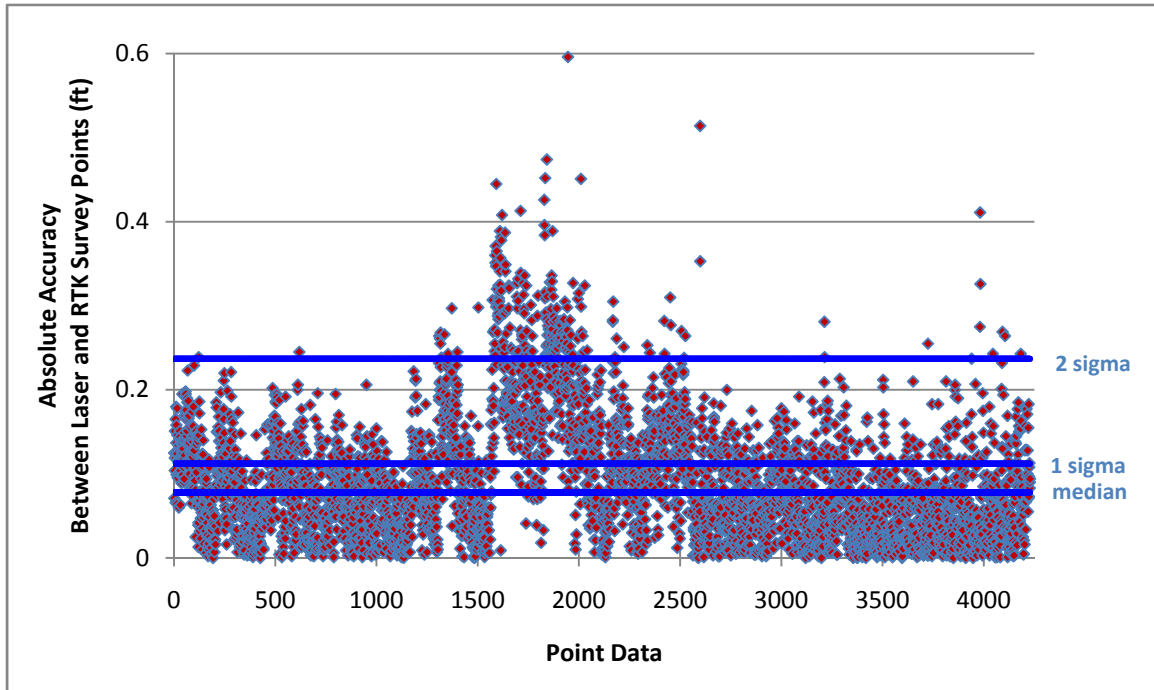


Figure 9. Absolute Accuracy - Absolute deviation, based on hard surface points.



## 5.5 Projection/Datum and Units

|              |                    |                     |
|--------------|--------------------|---------------------|
|              | <b>Projection:</b> | Montana State Plane |
| <b>Datum</b> | <b>Vertical:</b>   | NAVD88 Geoid03      |
|              | <b>Horizontal:</b> | NAD83 (HARN)        |
|              | <b>Units:</b>      | U.S. Survey Feet    |

## 6. Orthophoto Processing and Results

The deliverables for the Flathead Basin study area include 4-band (Red, Green, Blue, Near Infrared) orthorectified imagery. These were collected and processed by 3Di West (GeoTerra Mapping Group) based out of Eugene, Oregon. The photo acquisition parameters are summarized in **Table 4**.

*Table 4. Photo acquisition parameters*

---

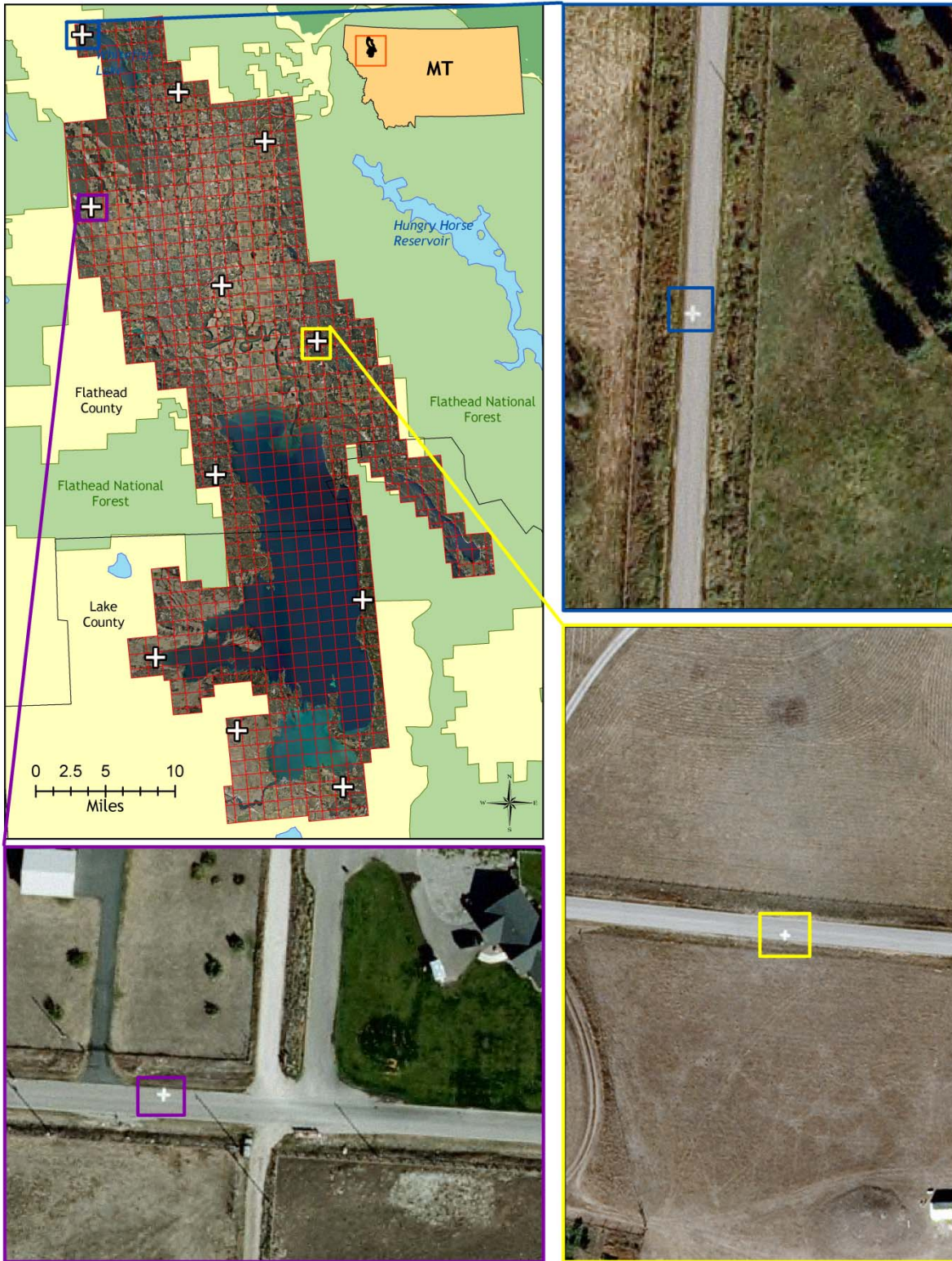
|                          |                       |
|--------------------------|-----------------------|
| Date:                    | September 23-25, 2009 |
|                          | Days 266- 268         |
| Camera:                  | Vexcel UltraCam XP    |
| Calibrated Focal Length: | 100.5 mm              |
| Photo Overlap:           | 60%                   |
| Photo Sidelap:           | 30%                   |
| Pixel Resolution:        | 1 foot                |

---

### 6.1 Processing

Surveyed aerial targets were used as ground control and aerial triangulation was performed to correctly place the imagery relative to the ground surface (**Table 5**). All imagery was orthorectified to the bare earth LiDAR surface. Individual image frames were combined into one seamless mosaic then subset into tiles to make the file size more manageable (**Figure 10**).

Figure 10. Flathead Basin orthophotograph tiles with survey control marker locations



Remote Sensing Data Acquisition and Processing: Flathead Basin, Montana

Prepared by Watershed Sciences, Inc.



## 6.2 Accuracy

The resulting orthoimagery has been compiled to meet National Map Accuracy Standards summarized below:

- Horizontal Accuracy: 1"=200' not more than 10% of all well-defined planimetric features are in error by more than 4.0'
- Optimal viewing at 1"=200'
  - Performing quality control or plotting images at scales larger than 1"=100' is not recommended.
  - Anomalies observable only at scales larger than 1"=100' are considered to fall outside the specifications of this project.

Table 5. Aerial Triangulation Report

| Precision - Root Mean Square Values of Residuals |             |          |          |           |          |
|--|-------------|----------|----------|-----------|----------|
| Point Type                                       | # of Points | X (feet) | Y (feet) | XY (feet) | Z (feet) |
| Tie Point  | 11,152      | 0.192    | 0.161    | 0.250     |          |
| Control  | 18          | 0.188    | 0.163    | 0.249     | 0.093    |

| Accuracy - Mean Value of Standard Deviation from Adjustment |          |           |          |
|---|----------|-----------|----------|
| X (feet)  | Y (feet) | XY (feet) | Z (feet) |
| 0.432   | 0.403    | 0.591     | 1.049    |

## 7. Hydrologically Enforced Terrain Model

Two versions of terrain models have been produced for the Flathead Basin study area. Both digital elevation models are created from a triangulated irregular network (TIN) of ground classified LiDAR points, however the second elevation model has hydrographic feature breaklines enforced.

3Di West (GeoTerra Mapping Group) collected breaklines for the Flathead basin study area using photogrammetric techniques. Appendix B describes the type and definition of each breakline collected. The photogrammetric breaklines were used to supplement the LiDAR data in creation of a hydrologically enforced ground model. Hard breaklines were draped to the elevation of the LiDAR derived ground model to co-register the elevation of the photogrammetric breakline with the LiDAR ground class. The stream breaklines were implemented as soft breaklines, and used to detect culverts. Points previously classified as ground above culverts in the LiDAR data were re-classed as non-ground, enabling stream channels to continue flow. Other breaklines, such as top of bank, were used to aid ground classification, and in areas where the LiDAR did not collect a ground point, ground points were added along the breakline.

Table 6. Breaklines collected for the Flathead study area

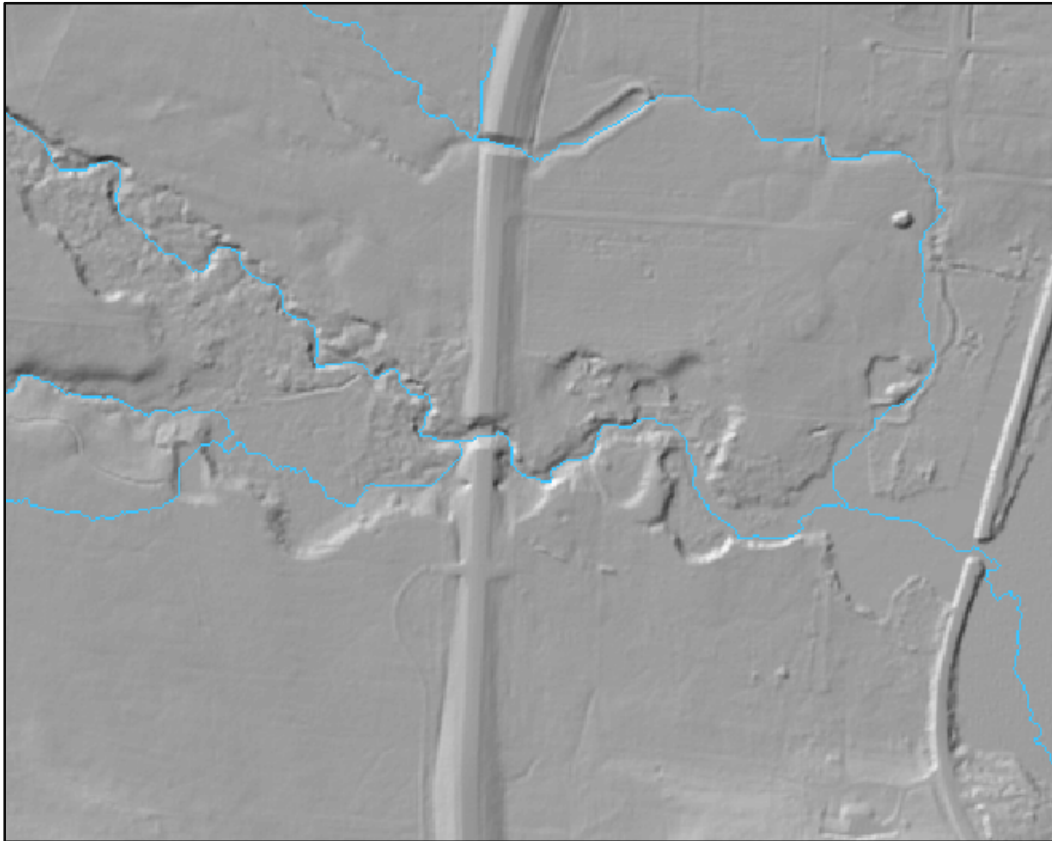
| Feature                         | Implementation           |
|---------------------------------|--------------------------|
| Hydro Break Earthen             | Aid ground classificaton |
| Hydro Canal                     | Aid ground classificaton |
| Hydro Dam Concrete              | Aid ground classificaton |
| Hydro Dam Earthen               | Aid ground classificaton |
| Hydro Ditch Bottom              | Aid ground classificaton |
| Hydro Ditch Top                 | Aid ground classificaton |
| Hydro Stream Bank Top           | Aid ground classificaton |
| Hydro Stream Interm             | Soft Breakline           |
| Hydro Stream Perennial          | Soft Breakline           |
| Hydro Stream Disappear PNT      | Provided as feature      |
| Hydro Waterbody                 | Soft Breakline           |
| Trans Airport Runway            | Hard Breakline           |
| Trans Airport Taxiway           | Hard Breakline           |
| Trans Road Paved Edge           | Hard Breakline           |
| Trans Road Unpaved Edge         | Hard Breakline           |
| Trans Road Private Paved Edge   | Hard Breakline           |
| Trans Road Private Unpaved Edge | Hard Breakline           |
| Breakline Misc                  | Aid ground classificaton |

The LiDAR DEM was hydrologically enhanced using the photogrammetrically derived breaklines. The breaklines were implemented in the LiDAR data model differently depending on the feature represented. The implementation for each feature is designed to provide the most accurate and hydrologically correct ground model:

- Hard breaklines (roads, paved edges, etc.) were incorporated into the TIN by enforcing triangle edges (adjacent to the breakline) to the elevation values derived from the photogrammetric breakline. This implementation corrected interpolation along the hard edge.
- For soft breaklines, the breaklines aided ground classification of LiDAR points along a particular feature as well as capturing areas of occlusion in the LiDAR point cloud (e.g. a large tree masking a floodplain terrace).
- Culverts were removed for the bare earth ground model to assist in enforcing stream junctions.
- Stream centerlines were inspected in the ground model. ArcHydro Tools 9 was run on ground models as a quality inspection of stream definition. **(Figure 11)** In areas where stream definition deviated from bare earth ground model and breaklines, LiDAR data was reexamined to provide increased detail (adding or subtracting appropriate ground classified points).

The resulting TIN was then converted into an ESRI grid at a 6 foot pixel resolution as per the contract.

*Figure 11. ArcHydro Tools 9 Stream Direction laid over LiDAR bare earth hillshade*

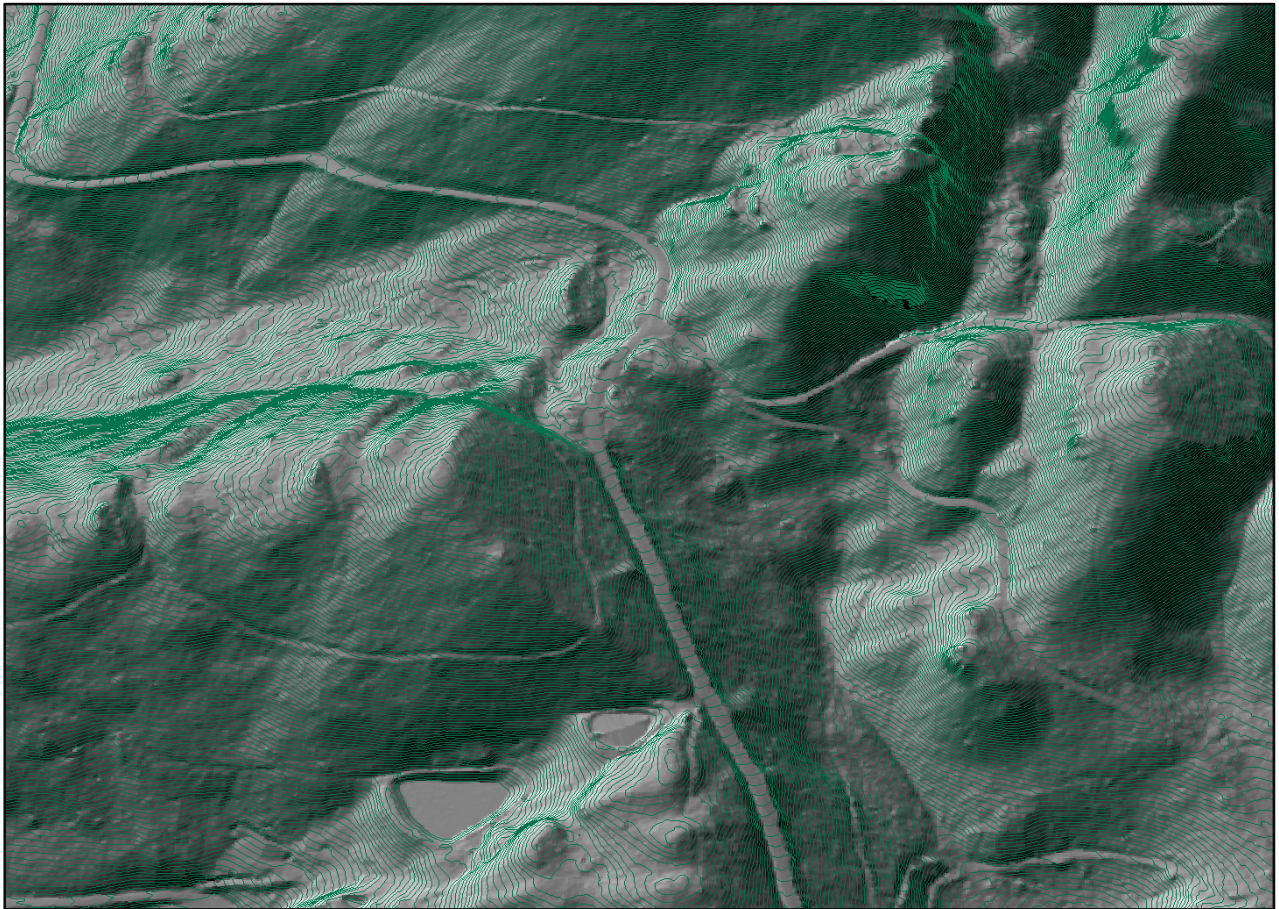




## 8. Contours

Contour key points were classed out of the ground model every 10 feet to provide more manageable dataset to work with (provided no significant change in Z). Contours were produced through TerraModeler with a Z tolerance of .33 feet. Contours were output in .dxf file format and have been converted to an ESRI feature class. The same breakline rules and resulting ground class for the hydrologically enforced ground model were used as the basis for contour creation.

*Figure 12. 2ft contours displayed over LiDAR bare earth hillshade*



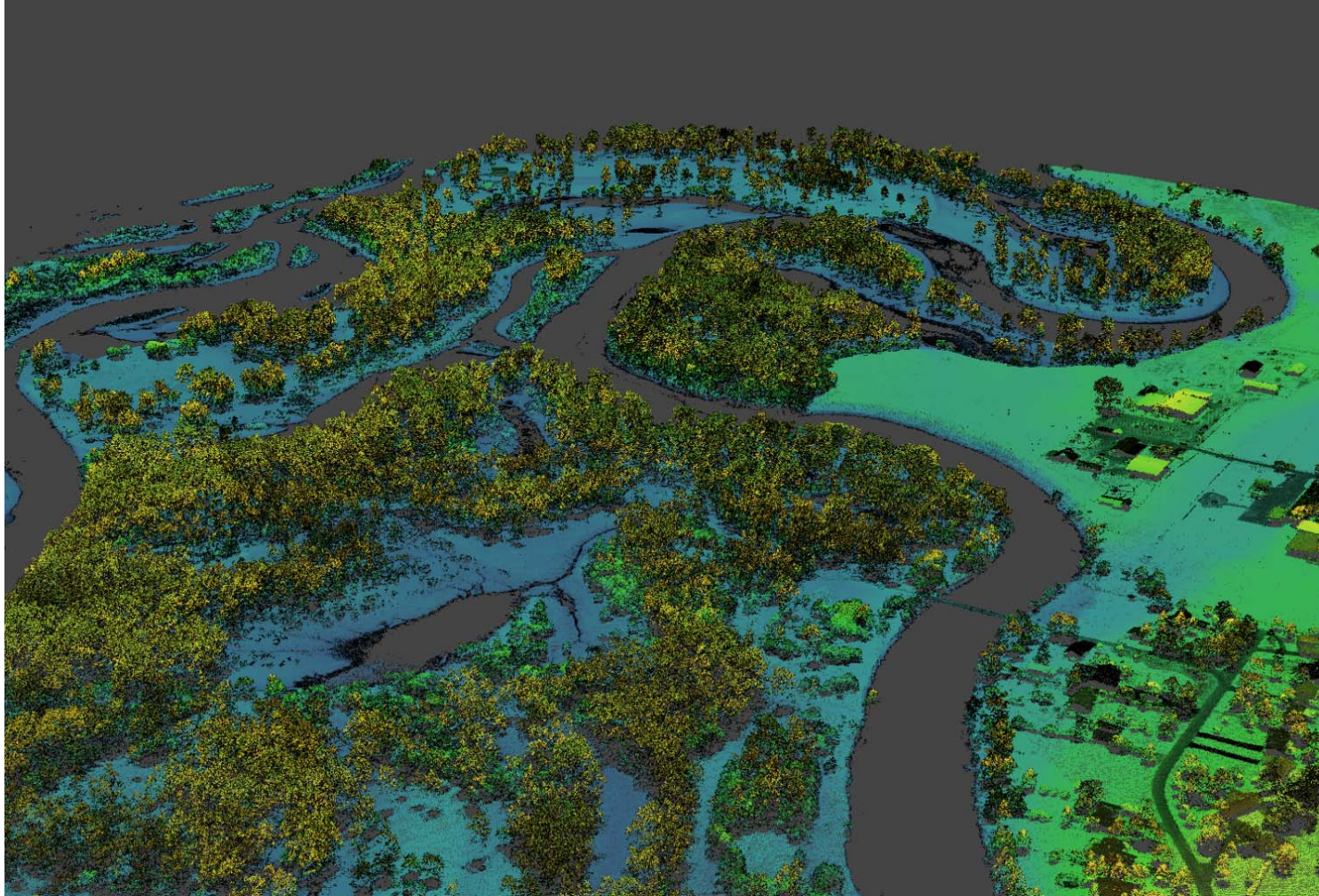
## 9. Deliverables

|                     |  |
|---------------------|--|
| <b>Point Data:</b>  | <ul style="list-style-type: none"> <li>• All Returns (Las v. 1.2 format, with attributes X,Y,Z, Return Intensity, Return Number, Point Classification, Number of Returns, Scan Angle, GPS Time)</li> <li>• Ground Classified Returns (Las v. 1.2 format, with attributes X,Y,Z, Return Intensity, Return Number, Point Classification, Number of Returns, Scan Angle, GPS Time)</li> </ul>   |
| <b>Vector Data:</b> | <ul style="list-style-type: none"> <li>• AOI boundary and tiling area, ESRI Geodatabase feature class</li> <li>• Contour Index and 2 ft. contours, ESRI Geodatabase feature class</li> <li>• Breaklines, ESRI Geodatabase feature class polyline Z format</li> <li>• DEM Tiling Index, ESRI Geodatabase feature class</li> <li>• Orthoimagery Tiling Index, ESRI Geodatabase feature class</li> <li>• Orthoimagery Flight Exposures, ESRI Geodatabase feature class</li> <li>• <i>Updated Roads Layer for survey area, ESRI geodatabase, provided by 3Di(value added product not in contract)</i></li> </ul>   |
| <b>Raster Data:</b> | <ul style="list-style-type: none"> <li>• Elevation Models             <ul style="list-style-type: none"> <li>• Bare earth DEM, 3-ft resolution, ESRI Grid format</li> <li>• Bare earth DEM with breaklines enforced, 6-ft resolution, ESRI Grid format</li> </ul> </li> <li>• Orthophotos             <ul style="list-style-type: none"> <li>• Compressed mosaic (MrSid format 1-ft resolution)</li> <li>• Compressed tiles (MrSid format 1-ft resolution)</li> <li>• Uncompressed tiles (GeoTIFF with worldfile 1-ft resolution)</li> <li>• Compressed near infrared tiles (MrSid format 1-ft resolution)</li> <li>• Compressed near infrared mosaic (MrSid format 1-ft resolution)</li> <li>• Uncompressed near infrared tiles (GeoTIFF with worldfile 1-ft resolution)</li> </ul> </li> <li>• Raw 4-Band Imagery (Tiff format)</li> </ul> |
| <b>Data Report:</b> | <ul style="list-style-type: none"> <li>• Full report containing introduction, methodology, and accuracy</li> </ul>   |



## 10. Selected Images

*Figure 13. 3-D point cloud looking southeast over the Flathead River just east of Kalispell, MT. (same approximate view as cover image)*

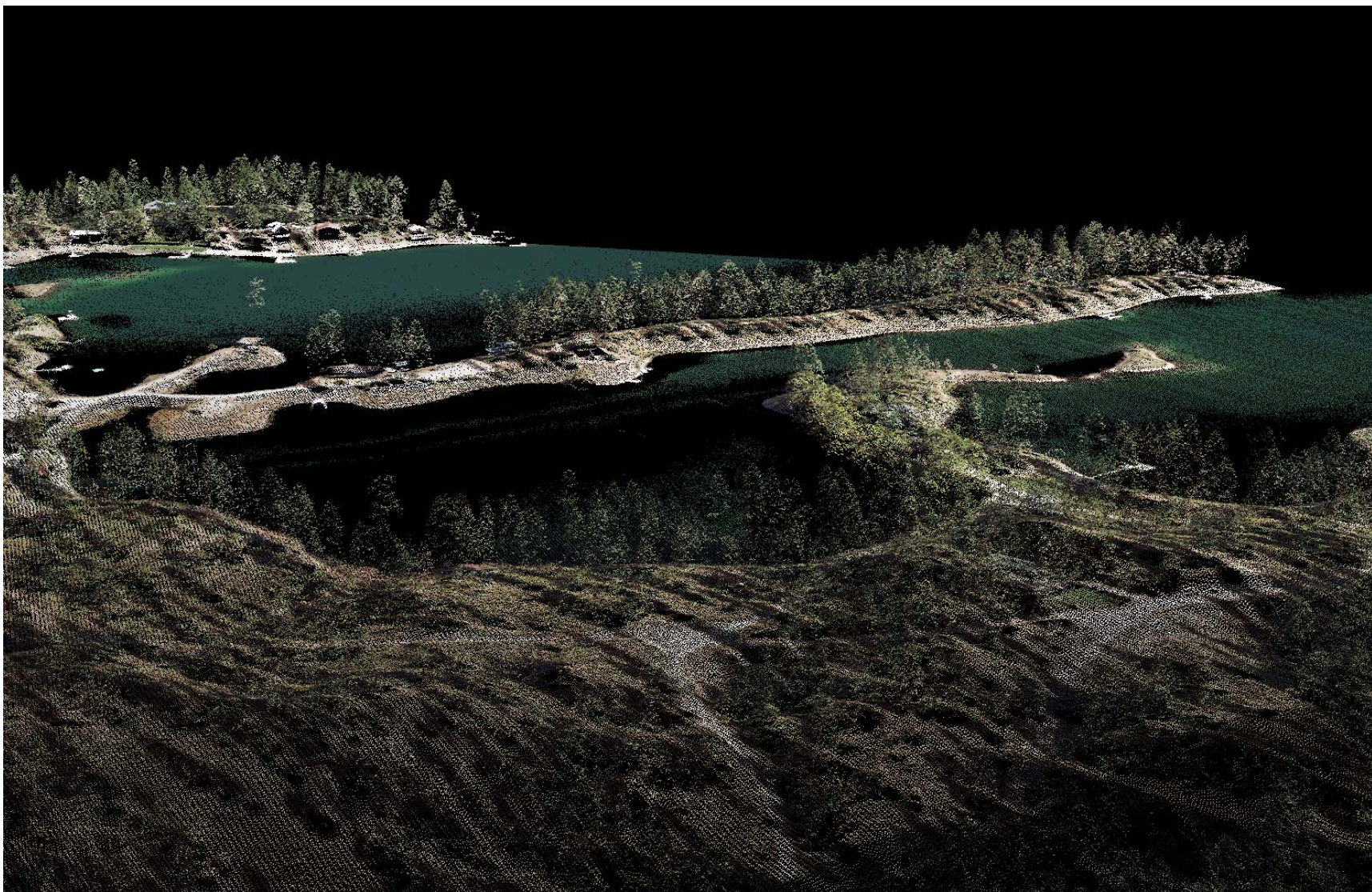


Remote Sensing Data Acquisition and Processing: Flathead Basin, Montana

Prepared by Watershed Sciences, Inc.



*Figure 14. 3-D point cloud looking southeast over Blackie's Bay, southeast of Creston, Mt. (same approximate view as cover image)*



**Remote Sensing Data Acquisition and Processing: Flathead Basin, Montana**

*Prepared by Watershed Sciences, Inc.*



*Figure 15. 3-D point cloud looking southwest over Bigfork dam on the Swan River. (colored by orthophotograph)*

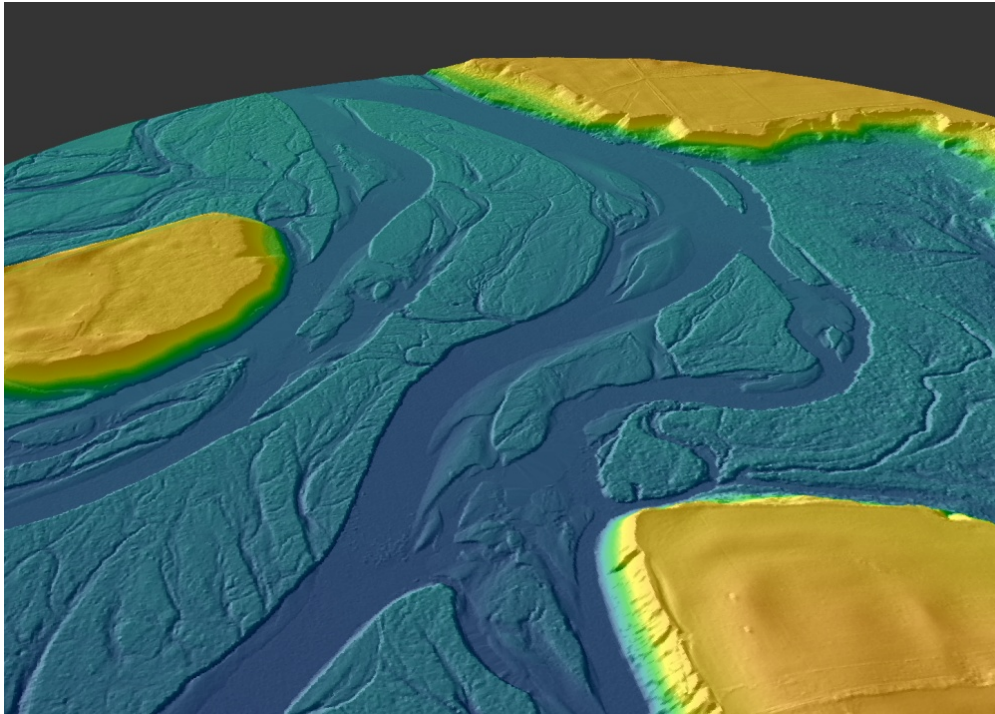


Remote Sensing Data Acquisition and Processing: Flathead Basin, Montana

Prepared by Watershed Sciences, Inc.



*Figure 16. Looking northwest over the Flathead River just northeast of Rose Crossing, MT. (top image is derived from ground-classified LiDAR points, middle image is derived from orthophotographs draped over highest hit LiDAR points, bottom image is derived from near infrared orthophotographs draped over highest hit LiDAR points)*



Remote Sensing Data Acquisition and Processing: Flathead Basin, Montana

Prepared by Watershed Sciences, Inc.



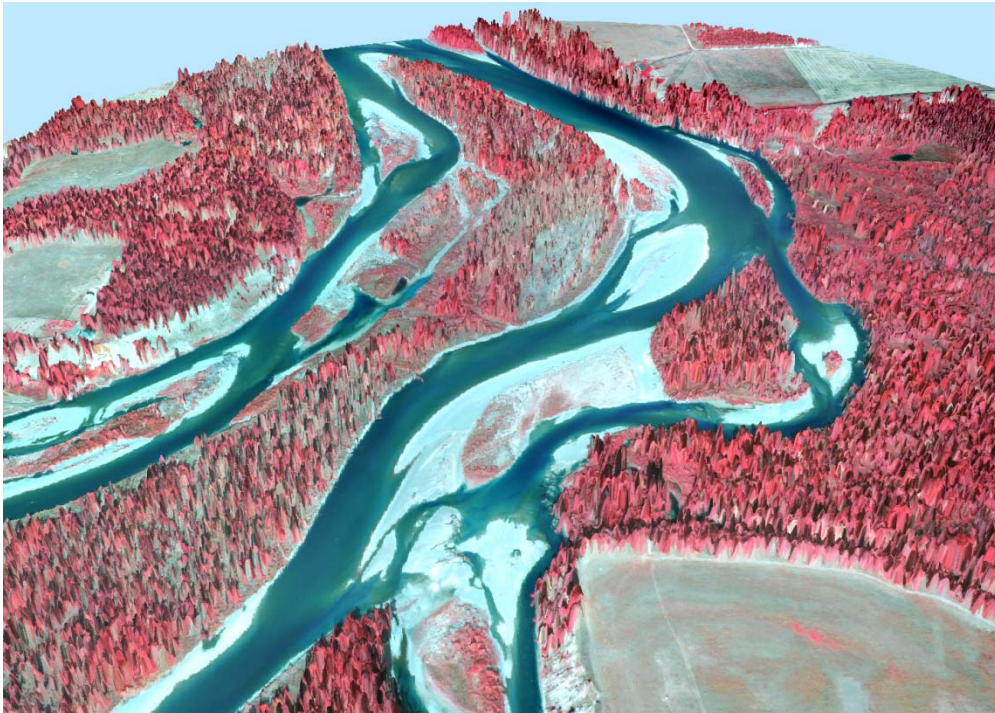
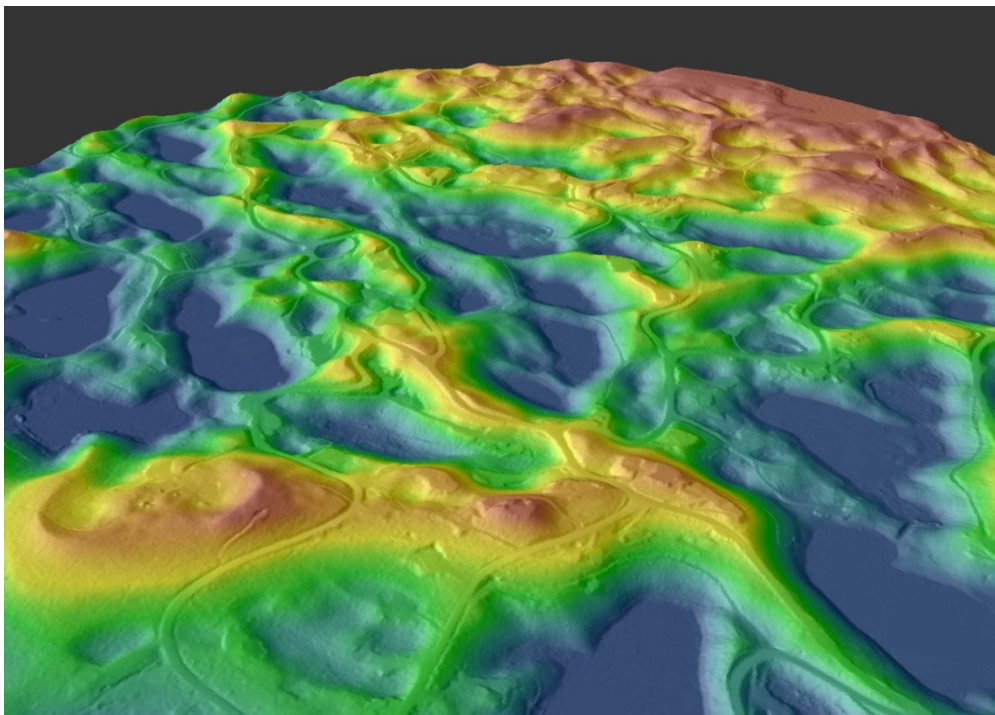


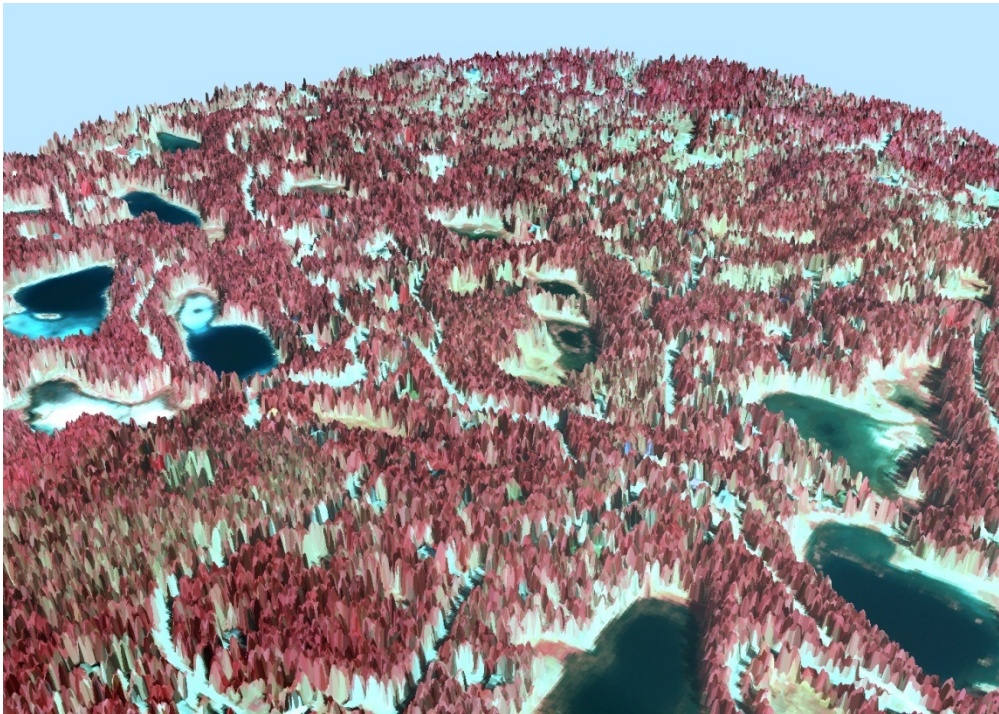
*Figure 17. Looking northeast from the northeast corner of Plummers Lake just east of Creston, Mt. (top image is derived from ground-classified LiDAR points, middle image is derived from orthophotographs draped over highest hit LiDAR points, bottom image is derived from near infrared orthophotographs draped over highest hit LiDAR points)*



Remote Sensing Data Acquisition and Processing: Flathead Basin, Montana

Prepared by Watershed Sciences, Inc.





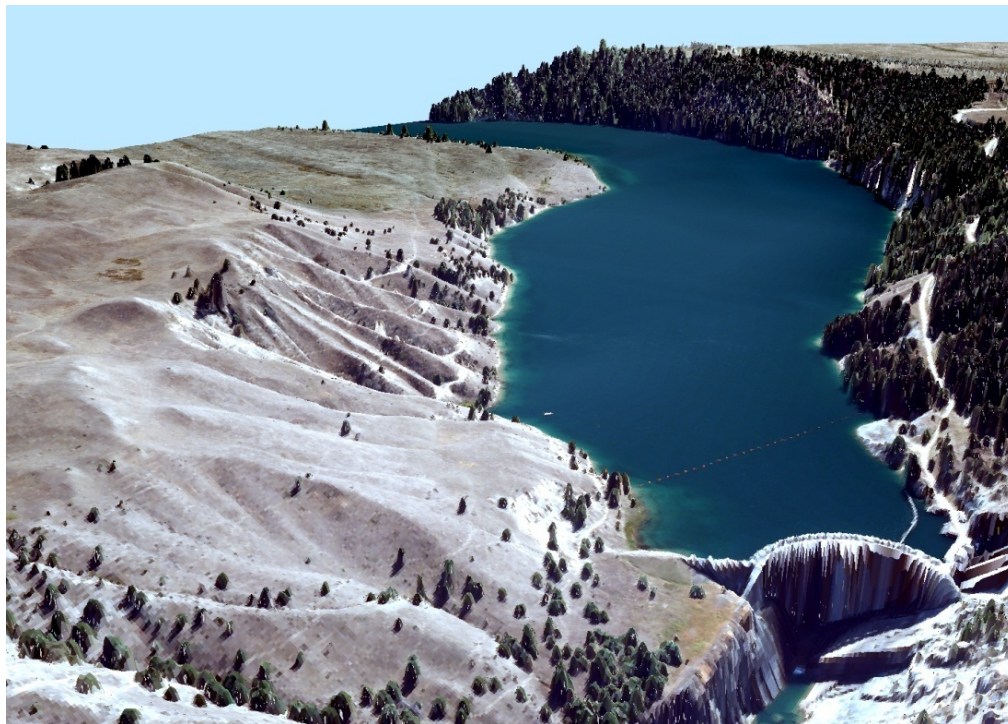
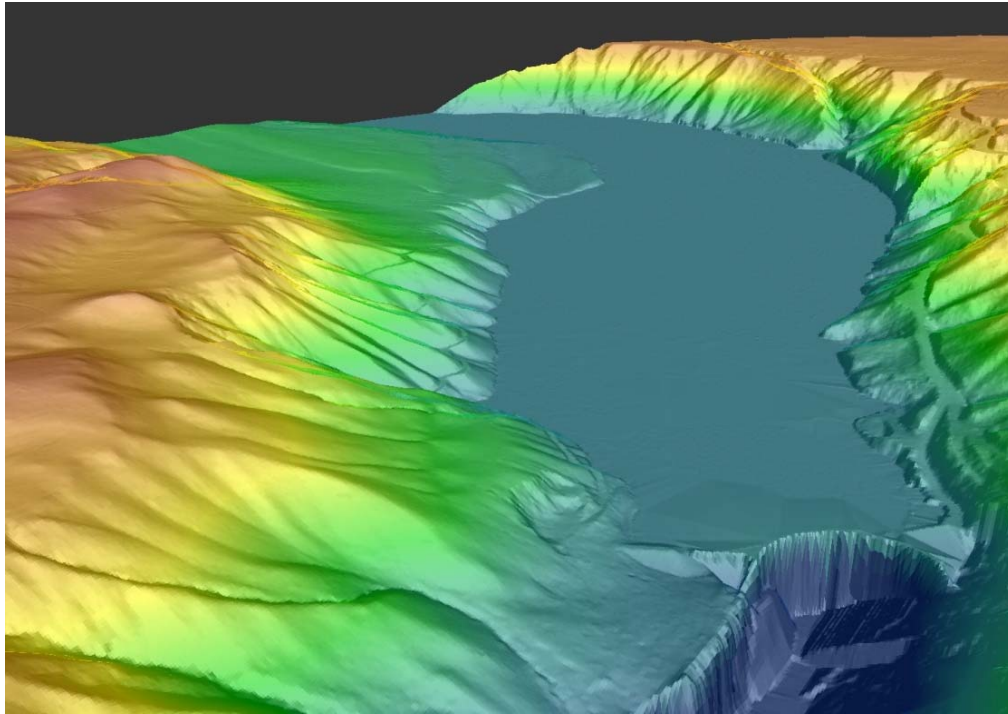
---

Remote Sensing Data Acquisition and Processing: Flathead Basin, Montana

*Prepared by Watershed Sciences, Inc.*



*Figure 18. Looking southeast over Kerr Dam (top image is derived from ground-classified LiDAR points, middle image is derived from orthophotographs draped over highest hit LiDAR points, bottom image is derived from near infrared orthophotographs draped over highest hit LiDAR points)*



Remote Sensing Data Acquisition and Processing: Flathead Basin, Montana

Prepared by Watershed Sciences, Inc.

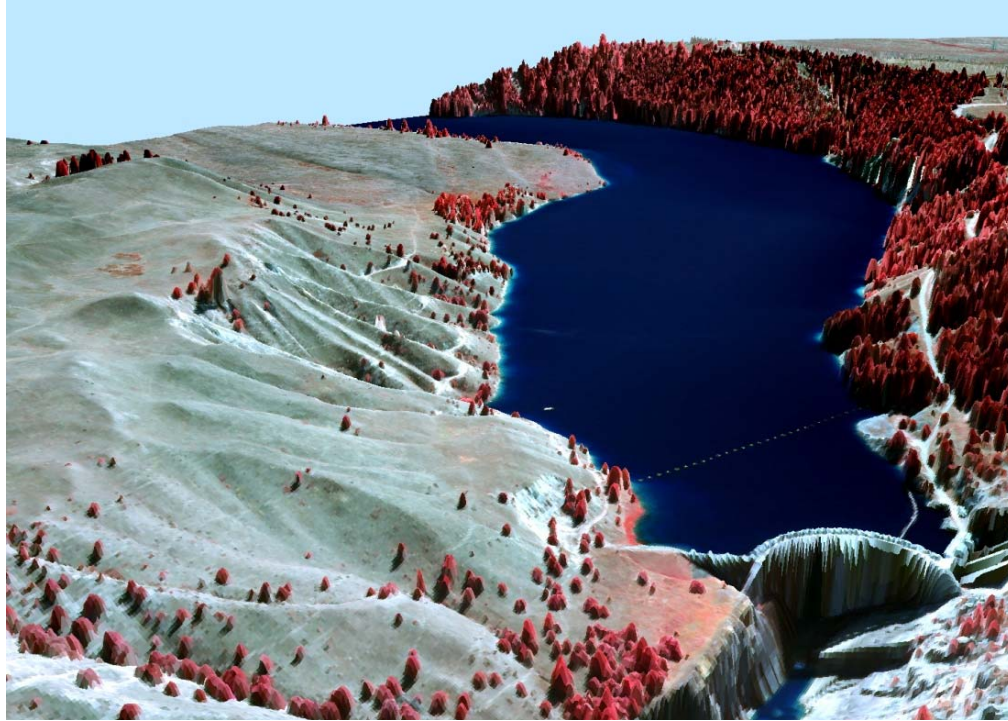
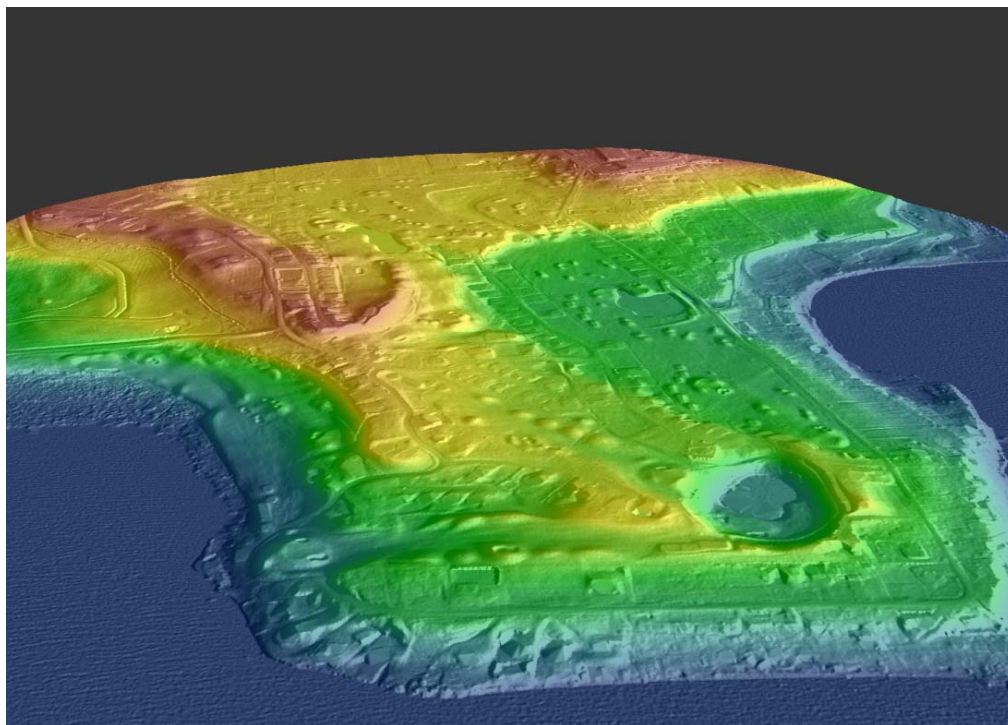


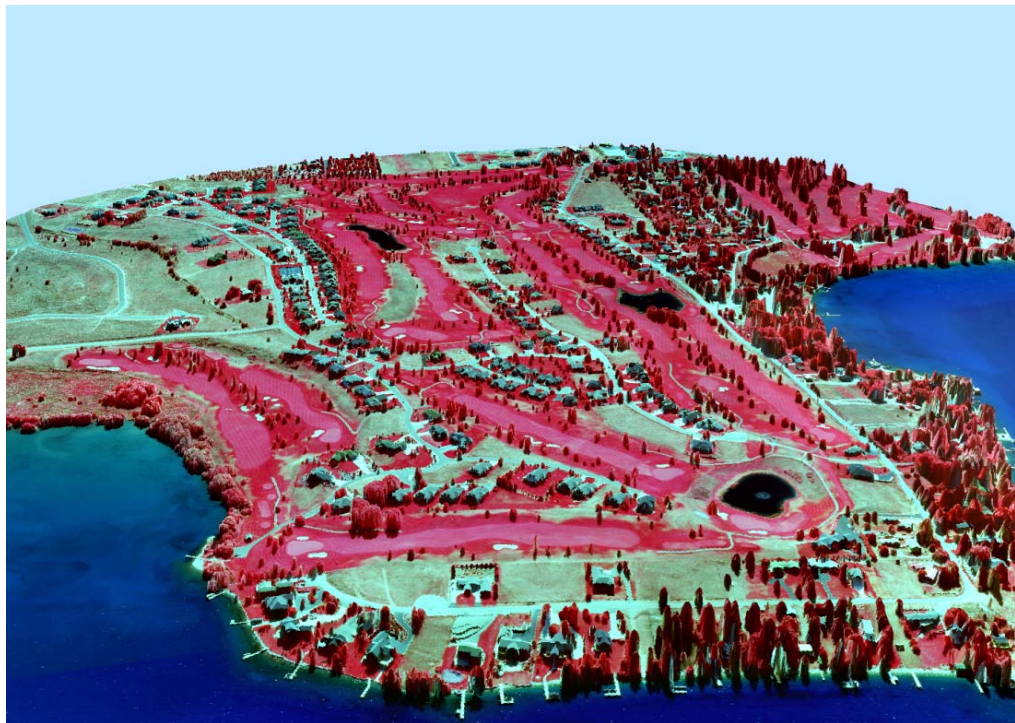
*Figure 19. Looking southwest over Polson Bay Golf Club (top image is derived from ground-classified LiDAR points, middle image is derived from orthophotographs draped over highest hit LiDAR points, bottom image is derived from near infrared orthophotographs draped over highest hit LiDAR points)*



Remote Sensing Data Acquisition and Processing: Flathead Basin, Montana

Prepared by Watershed Sciences, Inc.





Remote Sensing Data Acquisition and Processing: Flathead Basin, Montana

Prepared by Watershed Sciences, Inc.

## 11. Glossary

**1-sigma ( $\sigma$ ) Absolute Deviation:** Value for which the data are within one standard deviation (approximately 68<sup>th</sup> percentile) of a normally distributed data set.

**2-sigma ( $\sigma$ ) Absolute Deviation:** Value for which the data are within two standard deviations (approximately 95<sup>th</sup> percentile) of a normally distributed data set.

**Root Mean Square Error (RMSE):** A statistic used to approximate the difference between real-world points and the LiDAR points. It is calculated by squaring all the values, then taking the average of the squares and taking the square root of the average.

**Pulse Rate (PR):** The rate at which laser pulses are emitted from the sensor; typically measured as thousands of pulses per second (kHz).

**Pulse Returns:** For every laser pulse emitted, the Leica ALS 50 Phase II system can record *up to four* wave forms reflected back to the sensor. Portions of the wave form that return earliest are the highest element in multi-tiered surfaces such as vegetation. Portions of the wave form that return last are the lowest element in multi-tiered surfaces.

**Accuracy:** The statistical comparison between known (surveyed) points and laser points. Typically measured as the standard deviation (sigma,  $\sigma$ ) and root mean square error (RMSE).

**Intensity Values:** The peak power ratio of the laser return to the emitted laser. It is a function of surface reflectivity.

**Data Density:** A common measure of LiDAR resolution, measured as points per square meter.

**Spot Spacing:** Also a measure of LiDAR resolution, measured as the average distance between laser points.

**Nadir:** A single point or locus of points on the surface of the earth directly below a sensor as it progresses along its flight line.

**Scan Angle:** The angle from nadir to the edge of the scan, measured in degrees. Laser point accuracy typically decreases as scan angles increase.

**Overlap:** The area shared between flight lines, typically measured in percents; 100% overlap is essential to ensure complete coverage and reduce laser shadows.

**DTM / DEM:** These often-interchanged terms refer to models made from laser points. The digital elevation model (DEM) refers to all surfaces, including bare ground and vegetation, while the digital terrain model (DTM) refers only to those points classified as ground.

**Real-Time Kinematic (RTK) Survey:** GPS surveying is conducted with a GPS base station deployed over a known monument with a radio connection to a GPS rover. Both the base station and rover receive differential GPS data and the baseline correction is solved between the two. This type of ground survey is accurate to 1.5 cm or less.

## 12. Citations

Soininen, A. 2004. TerraScan User's Guide. TerraSolid.



## Appendix A

### LiDAR accuracy error sources and solutions:

| Type of Error             | Source                       | Post Processing Solution                    |
|---------------------------|------------------------------|---|
| GPS<br>(Static/Kinematic) | Long Base Lines              | None  |
|                           | Poor Satellite Constellation | None  |
|                           | Poor Antenna Visibility      | Reduce Visibility Mask                      |
| Relative Accuracy         | Poor System Calibration      | Recalibrate IMU and sensor offsets/settings |
|                           | Inaccurate System            | None  |
| Laser Noise               | Poor Laser Timing            | None  |
|                           | Poor Laser Reception         | None  |
|                           | Poor Laser Power             | None  |
|                           | Irregular Laser Shape        | None  |

### Operational measures taken to improve relative accuracy:

1. Low Flight Altitude: Terrain following is employed to maintain a constant above ground level (AGL). Laser horizontal errors are a function of flight altitude above ground (i.e., ~ 1/3000<sup>th</sup> AGL flight altitude).
2. Focus Laser Power at narrow beam footprint: A laser return must be received by the system above a power threshold to accurately record a measurement. The strength of the laser return is a function of laser emission power, laser footprint, flight altitude and the reflectivity of the target. While surface reflectivity cannot be controlled, laser power can be increased and low flight altitudes can be maintained.
3. Reduced Scan Angle: Edge-of-scan data can become inaccurate. The scan angle was reduced to a maximum of  $\pm 12^\circ$  from nadir, creating a narrow swath width and greatly reducing laser shadows from trees and buildings.
4. Quality GPS: Flights took place during optimal GPS conditions (e.g., 6 or more satellites and PDOP [Position Dilution of Precision] less than 3.0). Before each flight, the PDOP was determined for the survey day. During all flight times, a dual frequency DGPS base station recording at 1-second epochs was utilized and a maximum baseline length between the aircraft and the control points was less than 19 km (11.5 miles) at all times.
5. Ground Survey: Ground survey point accuracy (i.e. <1.5 cm RMSE) occurs during optimal PDOP ranges and targets a minimal baseline distance of 4 miles between GPS rover and base. Robust statistics are, in part, a function of sample size (n) and distribution. Ground survey RTK points are distributed to the extent possible throughout multiple flight lines and across the survey area.
6. 50% Side-Lap (100% Overlap): Overlapping areas are optimized for relative accuracy testing. Laser shadowing is minimized to help increase target acquisition from multiple scan angles. Ideally, with a 50% side-lap, the most nadir portion of one flight line coincides with the edge (least nadir) portion of overlapping flight lines. A minimum of 50% side-lap with terrain-followed acquisition prevents data gaps.
7. Opposing Flight Lines: All overlapping flight lines are opposing. Pitch, roll and heading errors are amplified by a factor of two relative to the adjacent flight line(s), making misalignments easier to detect and resolve.

## Appendix B

### Breakline Feature Descriptions

| Feature Name                    | Description   |
|---------------------------------|---|
| HYDRO_BREAK_EARTHEN             | Breakline defining where water flow potentially broken by man-made, earthen crossing with indistinct culvert present.   |
| HYDRO_CANAL                     | Breakline defining top of large, man-made, water-transport system.  |
| HYDRO_DAM_CONCRETE              | Breakline defining outline of concrete dam.   |
| HYDRO_DAM_EARTHEN               | Breakline defining breaks in stream flow due to apparent man-made earthen dam.  |
| HYDRO_DITCH_BOTTOM              | Breakline defining bottom of ditch where discernable  |
| HYDRO_DITCH_TOP                 | Breakline collected atop edge of stream bank where discernable.   |
| HYDRO_STREAM_BANK_TOP           | Breakline collected for lakes, reservoirs, holding ponds, etc... Collected as single water-line elevation reflected at time of flight. Delivered as closed polygon.   |
| HYDRO_STREAM_INTERM             | Breakline collected for an Intermittent stream (no water present at time of flight). Collected as a single breakline down middle of dry stream bed or at its lowest point if discernable.                             |
| HYDRO_STREAM_PERENNIAL          | Breakline collected for a Perrenial Stream (water present at time of flight). Collected at both edges of stream if greater than 8ft in width. Collected as single line at center of stream if less than 8ft in width. |
| HYDRO_STREAM_DISAPPEAR_PNT      | Breakline defining where water flow potentially broken by with no discernable continuation.   |
| HYDRO_WATERBODY                 | Breakline collected for lakes, reservoirs, holding ponds, etc... Collected as single water-line elevation reflected at time of flight. Delivered as closed polygon.   |
| TRANS_AIRPORT_RUNWAY            | Breakline collected at edge of paved runway.  |
| TRANS_AIRPORT_TAXIWAY           | Breakline collected at edge of paved taxiways, aprons or parking areas.   |
| TRANS_ROAD_PAVED_EDGE           | Breakline collected at edge of paved road.  |
| TRANS_ROAD_UNPAVED_EDGE         | Breakline collected at top edge of unpaved private road bed.  |
| TRANS_ROAD_PRIVATE_PAVED_EDGE   | Breakline collected at edge of paved road. Collected per existing Lake County Road Centerline file.   |
| TRANS_ROAD_PRIVATE_UNPAVED_EDGE | Breakline collected at edge of unpaved private road. Collected per existing Lake County Road Centerline file.   |
| BREAKLINE_MISC                  | Additional breaklines collected to better define sharp breaks in terrain; ex: top edge of cliff   |

## Appendix C

### Montana PLS verification



---

#### Flathead and Lake County LiDAR Control December 15, 2009

River Design Group, Inc. has completed the required control survey necessary to establish horizontal and vertical coordinates for the Flathead County LiDAR Acquisition.

The following established positions were utilized in this survey.

##### NGS CORS (continuously operating reference stations)

1. **MTFV** - located in Kalispell, MT.
2. **PLS6** - Located in Polson, MT

##### NGS Vertical Monuments

1. **F442** - as described on NGS Datasheet
2. **K443** - as described on NGS Datasheet
3. **Z443** - as described on NGS Datasheet
4. **A444** - as described on NGS Datasheet
5. **A507** - as described on NGS Datasheet
6. **Whitefish** - as described on NGS Datasheet

##### Newly established Control Monuments

1. **STUMPTOWN**
  - established by NW Chapter Marls for 2009 Height MOD
  - Position to be published by NGS in 2010
2. **STUMPTOWN secondary**
  - established as a redundant GPS Position
3. **F442 secondary**
  - established as a redundant GPS Position
4. **FERNDALÉ primary**
  - established as Primary GPS Position due to lack of existing monumentation
5. **FERNDALÉ secondary**
  - established as a redundant GPS Position
6. **A507 secondary**

##### Aerial Triangulation Pre-Marks

- Painted Targets SV 1 to SV 12

#### DATA COLLECTION METHODOLOGY

Utilizing Trimble R8 survey grade GPS receivers, multiple redundant long (> 4 hour) GPS static observations were measured on each newly established control point with concurrent and equal length static observations on the NGS vertical monuments (K442, K443, Z443, A444 & A507). Elevations were established for newly set monuments via differential leveling utilizing a Topcon DL103 Digital Level.

##### NOTES:

1. STUMPTOWN and STUMPTOWN secondary elevations were established via Differential Leveling from WHITEFISH.
2. FERNDALÉ and FERNDALÉ secondary are Geoid03 quality elevations due to lack of 3d monumentation in the vicinity.

## STATIC OBSERVATION PROCESSING METHODOLOGY

The static occupations discussed above were processed and adjusted against the two NGS CORS positions utilizing Trimble Geomatics Office ver. 1.63. These solutions were used to provide survey grade horizontal solutions and geoid03 vertical solutions. The geoid03 solutions for K442, K443, Z443, A444 & A507 were then compared to the published vertical positions reported by NGS. *(This is necessary to analyze these vertical deltas to find the error in local geoid heights and to isolate possible disturbed or inaccurate vertical monuments.)*

## FINAL GEODETIC COORDINATES

**Horizontal Datum:** North American Datum of 1983 (CORS)  
**Horizontal Projection:** Montana State Plane  
**Horizontal Units:** (ussft) United States Survey Feet  
**Vertical Datum:** NAVD88 North American Vertical Datum of 1988 - Geoid03  
**Vertical Units:** (ussft) United States Survey Feet

| sta                     | northing (ussft) | easting (ussft) | elevation (ussft) |
|-------------------------|------------------|-----------------|-------------------|
| WF Airport              | 1552499.1290     | 801687.2900     | 3050.34           |
| WF Airport (secondary)  | 1552480.1200     | 801677.0340     | 3050.89           |
| NGS F 442               | 1445038.2650     | 807979.1550     | 2912.34           |
| NGS F442 (secondary)    | 1445053.8060     | 807984.1430     | 2912.70           |
| Ferndale (primary)      | 1417603.0100     | 867473.0000     | 3066.99           |
| ferndale (secondary)    | 1417607.4730     | 867414.8780     | 3066.93           |
| K 443                   | 1343787.2200     | 782200.7330     | 2944.47           |
| NGS Z 443               | 1304227.4640     | 809124.0600     | 3094.62           |
| NGS A 444               | 1300323.8200     | 811816.0030     | 2974.95           |
| SV-08                   | 1354932.8400     | 858174.7720     | 2963.60           |
| SV-12                   | 1284967.4150     | 843888.0940     | 2935.59           |
| SV-11                   | 1310103.5790     | 805974.2170     | 3428.13           |
| SV-10                   | 1340835.2250     | 777899.7060     | 2926.52           |
| SV-02                   | 1553701.7850     | 807116.3790     | 3100.05           |
| SV-03                   | 1531877.2040     | 838041.5110     | 3091.56           |
| SV-04                   | 1513583.3060     | 769979.7910     | 3137.69           |
| SV-01                   | 1578930.4900     | 772913.1370     | 3006.58           |
| SV-09                   | 1373403.8660     | 902655.4200     | 3081.63           |
| SV-06                   | 1454510.8710     | 850466.1170     | 3035.35           |
| SV-07                   | 1407708.7490     | 807188.2310     | 3082.46           |
| SV-05                   | 1478941.7910     | 816425.4380     | 2936.25           |
| NGS A507<br>(SECONDARY) | 1513663.5540     | 813440.1300     | 2963.23           |
| NGS A 507               | 1514631.6270     | 813273.0640     | 2967.76           |

| sta                     | latitude         | longitude         | height (ussft) |
|-------------------------|------------------|-------------------|----------------|
| WF Airport              | 48°24'36.47915"N | 114°18'30.39731"W | 2997.69        |
| WF Airport (secondary)  | 48°24'36.28566"N | 114°18'30.53178"W | 2998.27        |
| NGS F 442               | 48°07'01.42707"N | 114°15'20.60613"W | 2860.07        |
| NGS F442 (secondary)    | 48°07'01.58321"N | 114°15'20.54662"W | 2860.43        |
| Ferndale (primary)      | 48°03'05.74842"N | 114°00'21.65367"W | 3015.84        |
| ferndale (secondary)    | 48°03'05.75942"N | 114°00'22.51189"W | 3015.79        |
| K 443                   | 47°50'08.06192"N | 114°20'07.84518"W | 2893.19        |
| NGS Z 443               | 47°43'54.37511"N | 114°12'58.82530"W | 3043.57        |
| NGS A 444               | 47°43'17.49697"N | 114°12'16.06767"W | 2923.95        |
| SV-08                   | 47°52'42.73083"N | 114°01'45.00981"W | 2913.14        |
| SV-12                   | 47°41'04.86871"N | 114°04'14.44625"W | 2885.39        |
| SV-11                   | 47°44'50.41685"N | 114°13'50.03322"W | 3377.11        |
| SV-10                   | 47°49'36.34566"N | 114°21'08.11760"W | 2875.37        |
| SV-02                   | 48°24'51.60839"N | 114°17'11.14315"W | 3047.49        |
| SV-03                   | 48°21'34.95439"N | 114°09'14.19312"W | 3039.20        |
| SV-04                   | 48°17'53.63403"N | 114°25'43.28965"W | 3085.20        |
| SV-01                   | 48°28'39.21779"N | 114°26'00.83321"W | 2954.67        |
| SV-09                   | 47°56'09.69683"N | 113°51'08.24309"W | 3032.38        |
| SV-06                   | 48°08'59.77185"N | 114°05'03.44287"W | 2983.26        |
| SV-07                   | 48°00'53.08824"N | 114°14'58.89186"W | 3030.88        |
| SV-05                   | 48°12'40.56239"N | 114°13'46.47019"W | 2883.23        |
| NGS A507<br>(SECONDARY) | 48°18'20.91574"N | 114°15'01.56654"W | 2910.03        |
| NGS A 507               | 48°18'30.35446"N | 114°15'04.90241"W | 2914.56        |



| CONTROL PT             | monuments             | gps quality     | vertical method     |
|------------------------|-----------------------|-----------------|---------------------|
| WF Airport             | steel rod in casement | NAVD88 control  | differential level  |
| WF Airport (secondary) | 2" alum cap (rdg)     | NAVD88 control  | differential level  |
| NGS F 442              | NGS (per datasheet)   | NAVD88 control  | NGS control         |
| NGS F442 (secondary)   | 2" alum cap (rdg)     | NAVD88 control  | differential level  |
| Ferndale (primary)     | 2" alum cap (rdg)     | NAVD88 geoid 03 | geoid03 observation |
| ferndale (secondary)   | 2" alum cap (rdg)     | NAVD88 geoid 03 | geoid03 observation |
| K 443                  | NGS (per datasheet)   | NAVD88 control  | NGS control         |
| NGS Z 443              | NGS (per datasheet)   | NAVD88 control  | NGS control         |
| NGS A 444              | NGS (per datasheet)   | NAVD88 control  | NGS control         |
| SV-08                  | pk nail-brass washer  | NAVD88 geoid 03 | geoid03 observation |
| SV-12                  | pk nail-brass washer  | NAVD88 geoid 03 | geoid03 observation |
| SV-11                  | pk nail-brass washer  | NAVD88 geoid 03 | geoid03 observation |
| SV-10                  | pk nail-brass washer  | NAVD88 geoid 03 | geoid03 observation |
| SV-02                  | pk nail-brass washer  | NAVD88 geoid 03 | geoid03 observation |
| SV-03                  | pk nail-brass washer  | NAVD88 geoid 03 | geoid03 observation |
| SV-04                  | pk nail-brass washer  | NAVD88 geoid 03 | geoid03 observation |
| SV-01                  | pk nail-brass washer  | NAVD88 geoid 03 | geoid03 observation |
| SV-09                  | pk nail-brass washer  | NAVD88 geoid 03 | geoid03 observation |
| SV-06                  | pk nail-brass washer  | NAVD88 geoid 03 | geoid03 observation |
| SV-07                  | pk nail-brass washer  | NAVD88 geoid 03 | geoid03 observation |
| SV-05                  | pk nail-brass washer  | NAVD88 geoid 03 | geoid03 observation |
| NGS A507 (SECONDARY)   | 2" alum cap (rdg)     | NAVD88 control  | differential level  |
| NGS A 507              | NGS (per datasheet)   | NAVD88 control  | geoid03 observation |

### LiDAR Absolute Accuracy

River Design Group collected 1000 sample points to test the accuracy of the final LiDAR surface. Each of these points were classified by average ground cover and land type and sampled against the Final Surface.

The Results of this analysis are as shown below:

|                            | asphalt | Cat tails | concrete | cultivated fields | drain rock | grass | grass lawn | gravel | natural fields | packed dirt | shrubs |
|----------------------------|---------|-----------|----------|-------------------|------------|-------|------------|--------|----------------|-------------|--------|
| $\Delta$ Average Elevation | -0.04   | 1.00      | -0.12    | 0.12              | 0.10       | 0.21  | 0.07       | 0.07   | 0.26           | 0.05        | 0.26   |
| $\Delta$ Minimum Elevation | -0.33   | 0.27      | -0.57    | -0.07             | -0.19      | -0.19 | -0.23      | -0.29  | -0.36          | -0.35       | -0.66  |
| $\Delta$ Maximum Elevation | 0.27    | 1.66      | 0.34     | 0.41              | 0.28       | 0.62  | 0.37       | 0.44   | 0.94           | 0.46        | 0.94   |
| Average Magnitude          | 0.12    | 1.00      | 0.18     | 0.13              | 0.16       | 0.24  | 0.13       | 0.14   | 0.29           | 0.16        | 0.54   |
| Root Mean Square           | 0.14    | 1.04      | 0.23     | 0.16              | 0.18       | 0.28  | 0.16       | 0.18   | 0.36           | 0.20        | 0.57   |
| Standard Deviation         | 0.14    | 0.30      | 0.20     | 0.11              | 0.15       | 0.20  | 0.15       | 0.16   | 0.25           | 0.20        | 0.52   |



04 March 2010

Andrew P. Belski, PLS  
Montana Professional Land Surveyor 14731PLS

Date

**Montana Office**  
5098 Highway 93 South  
Whitefish, Montana 59937  
(406) 862-4927 • Fax (406) 862-4963

**Oregon Office**  
311 SW Jefferson Avenue  
Corvallis, Oregon 97333  
(541) 738-2920 • Fax (541) 758-8524

LiDAR Data Acquisition and Processing, Flathead Basin, Montana  
Prepared by Watershed Sciences, Inc.